

## ARTICLE

# FXYP protein isoforms differentially modulate human Na/K pump function

Dylan J. Meyer<sup>1</sup>, Sharan Bijlani<sup>1</sup>, Marilina de Sautu<sup>1</sup>, Kerri Spontarelli<sup>1</sup>, Victoria C. Young<sup>1</sup>, Craig Gatto<sup>2</sup>, and Pablo Artigas<sup>1</sup>

**Tight regulation of the Na/K pump is essential for cellular function because this heteromeric protein builds and maintains the electrochemical gradients for Na<sup>+</sup> and K<sup>+</sup> that energize electrical signaling and secondary active transport. We studied the regulation of the ubiquitous human  $\alpha 1\beta 1$  pump isoform by five human FXYP proteins normally located in muscle, kidney, and neurons. The function of Na/K pump  $\alpha 1\beta 1$  expressed in *Xenopus* oocytes with or without FXYP isoforms was evaluated using two-electrode voltage clamp and patch clamp. Through evaluation of the partial reactions in the absence of K<sup>+</sup> but presence of Na<sup>+</sup> in the external milieu, we demonstrate that each FXYP subunit alters the equilibrium between E1P(3Na) and E2P, the phosphorylated conformations with Na<sup>+</sup> occluded and free from Na<sup>+</sup>, respectively, thereby altering the apparent affinity for Na<sup>+</sup>. This modification of Na<sup>+</sup> interaction shapes the small effects of FXYP proteins on the apparent affinity for external K<sup>+</sup> at physiological Na<sup>+</sup>. FXYP6 distinctively accelerated both the Na<sup>+</sup>-deocclusion and the pump-turnover rates. All FXYP isoforms altered the apparent affinity for intracellular Na<sup>+</sup> in patches, an effect that was observed only in the presence of intracellular K<sup>+</sup>. Therefore, FXYP proteins alter the selectivity of the pump for intracellular ions, an effect that could be due to the altered equilibrium between E1 and E2, the two major pump conformations, and/or to small changes in ion affinities that are exacerbated when both ions are present. Lastly, we observed a drastic reduction of Na/K pump surface expression when it was coexpressed with FXYP1 or FXYP6, with the former being relieved by injection of PKA's catalytic subunit into the oocyte. Our results indicate that a prominent effect of FXYP1 and FXYP6, and plausibly other FXYPs, is the regulation of Na/K pump trafficking.**

## Introduction

All human cells need to build and maintain electrochemical gradients for Na<sup>+</sup> and K<sup>+</sup> across their plasma membrane in order to subsist. Such gradients are built exclusively by the Na/K pump (aka Na<sup>+</sup>/K<sup>+</sup>-ATPase), which, in its minimally functional form, comprises a large catalytic  $\alpha$  subunit (~100 kD) and a glycosylated  $\beta$  subunit (~55 kD).

Because the Na<sup>+</sup> and K<sup>+</sup> gradients built by the Na/K pump are essential for diverse cellular functions, such as excitability or epithelial transport, it is logical that Na<sup>+</sup>/K<sup>+</sup> transport is tightly regulated. Thus, vertebrates express several  $\alpha$  ( $\alpha 1$ – $\alpha 4$ ) and  $\beta$  ( $\beta 1$ – $\beta 3$ ) isoforms in a tissue-specific, and often cell-specific, manner. The formation of various  $\alpha_x\beta_x$  pumps, each with unique kinetic properties (Blanco, 2005; Blanco et al., 1995; Crambert et al., 2000; DiFranco et al., 2015; Geering, 2008; Hilbers et al., 2016; Meyer et al., 2019; Stanley et al., 2015), provides cells with versatile Na/K pump activities for regulating their specific Na<sup>+</sup> and K<sup>+</sup> transport needs.

Despite the versatile pump functions offered by available  $\alpha_x\beta_x$  dimer combinations, the Na/K pump is found as a trimer in many tissues, owing to its association with a small, single-membrane-spanning FXYP protein (~8–20 kD; Geering, 2008). FXYP2 (the Na/K pump  $\gamma$  subunit) was the first FXYP identified in kidney (Forbush et al., 1978; Mercer et al., 1993). FXYP4 (corticosteroid hormone-induced factor; Attali et al., 1995) was also found in kidney, where its expression increases in response to corticosteroid hormone. FXYP1 (phospholemman; Palmer et al., 1991; Moorman et al., 1992) was found to be an important PKA and PKC protein target in the heart and skeletal muscle, and was later reported in brain and kidney (Arystarkhova et al., 2017; Feschenko et al., 2003). FXYP6 (phosphohippolin) and FXYP7 seem to be exclusive to the nervous system (Béguin et al., 2002; Delprat et al., 2007; Kadowaki et al., 2004), while FXYP3 (Mat-8; Morrison et al., 1995) and FXYP5 (dysadherin or related to ion channel; Ino et al., 2002) are

<sup>1</sup>Department of Cell Physiology and Molecular Biophysics, Center for Membrane Protein Research, Texas Tech University Health Sciences Center, Lubbock TX; <sup>2</sup>School of Biological Sciences, Illinois State University, Normal, IL.

Correspondence to Pablo Artigas: [pablo.artigas@ttuhsc.edu](mailto:pablo.artigas@ttuhsc.edu).

© 2020 Meyer et al. This article is distributed under the terms of an Attribution–Noncommercial–Share Alike–No Mirror Sites license for the first six months after the publication date (see <http://www.rupress.org/terms/>). After six months it is available under a Creative Commons License (Attribution–Noncommercial–Share Alike 4.0 International license, as described at <https://creativecommons.org/licenses/by-nc-sa/4.0/>).

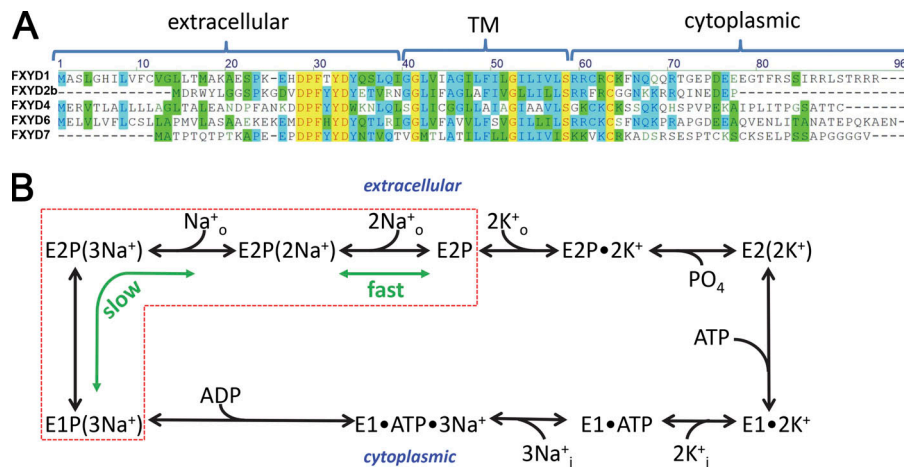


**Figure 1. FXYP amino acid sequence alignment and Na/K pump enzymatic cycle. (A)** Alignment of the five human FXYP isoforms studied in this work. Residues in the transmembrane (TM), cytoplasmic, and extracellular regions of the isoforms are indicated. **(B)** Post-Albers kinetic scheme of the Na/K pump cycle (clockwise forward direction). The pump alternates between two major conformations, E1 and E2, which can exist in dephosphorylated or phosphorylated (P) forms. Parentheses indicate ions occluded within the protein. Transitions within the red box produce transient charge movement: the release of the first Na<sup>+</sup> (forward cycle) or rebinding of the last Na<sup>+</sup> (backward cycle) during E1P(3Na<sup>+</sup>) ↔ E2P(2Na<sup>+</sup>) + Na<sup>+</sup> produces the slow transient charge movement, while the release of the last two Na<sup>+</sup> ions (forward cycle) or rebinding of the first two Na<sup>+</sup> ions (backward cycle) during E2P(2Na<sup>+</sup>) ↔ E2P + 2Na<sup>+</sup> produces fast charge movement.

expressed in several epithelia and appear to be up-regulated in certain cancers.

The physiological role of the FXYP proteins remains elusive. Geering's pioneering work (Geering, 2006; Geering, 2008) demonstrated that each FXYP protein induces small, yet distinct, changes to the function of α1β1 pumps expressed in *Xenopus laevis* oocytes, but studies using other preparations or experimental systems (ranging from cells to purified protein) have sometimes produced contradictory results. Many of these studies were performed using αβFXYP pumps formed from isoforms of different species, which may hinder experimental interpretation.

Here we use two-electrode voltage clamp (TEVC) and patch clamp to compare the effects of five human FXYP subunits (Fig. 1 A) on human α1β1 pumps when coexpressed in *Xenopus* oocytes. We observed that association of α1β1 with each FXYP isoform uniquely alters the Na/K pump's apparent affinities for transported ions, effects that are largely dictated by ion binding competition. We also found that each FXYP modifies the rate and proportion of slow transient charge movement that reflects the pump's transition between the phosphorylated forms of the two major Na/K pump conformations, E1P(3Na) and E2P (Fig. 1 B, dotted box). In addition, we describe the novel observation that FXYP1 and FXYP6 drastically reduced the surface expression of α1β1 pumps, a result indicating that a prominent mechanism for regulation of Na/K pump activity by FXYP1 and FXYP6 may be through Na/K pump trafficking, in line with recent proposals (Lin et al., 2013).

## Materials and methods

### Oocyte isolation

*Xenopus* oocytes were isolated in accordance with approved Texas Tech University Health Sciences Center Institutional Animal Care and Use Committee protocols, as described by Meyer et al. (2017). Briefly, oocyte lobes were cut and incubated with collagenase from *Clostridium histolyticum* (2 mg/ml, C2674; Sigma-Aldrich) for 1 h in an OR2 solution containing (in mM)

82.5 NaCl, 1 MgCl<sub>2</sub>, 2 KCl, and 5 HEPES, titrated to pH 7.5 with NaOH. The oocytes were then rinsed, incubated three times in OR2 + 2 mM CaCl<sub>2</sub> for 45 min, and transferred to standard oocyte solution (~220 mOsm/kg) comprising (in mM) 100 NaCl, 1 MgCl<sub>2</sub>, 2 KCl, 1.8 CaCl<sub>2</sub>, 5 HEPES, 2.5 pyruvic acid (Sigma-Aldrich), 1× antibiotic-antimycotic (Gibco), and 5% horse serum (Gibco), titrated to pH 7.5 with NaOH.

### Molecular biology

Plasmid DNA (pSD5 vector) containing human α1, human β1, or human FXYP cDNA was linearized using NdeI (for α1), NotI (for β1), BglII (for FXYP1, FXYP2b [one of two splice variants], FXYP6, and FXYP7), or PvuI (for FXYP4). Complementary RNA (cRNA) was transcribed in vitro with the SP6 mMessage machine kit (Ambion). Oocytes were injected with cRNA mixtures of α1:β1:FXYP<sub>x</sub> (75 ng α1 and 25 ng β1 or 75 ng α1, 25 ng β1, and 16.6 ng FXYP) and kept at 16°C for 3–6 d until recording.

The rodent α1 catalytic subunit is naturally more resistant to the inhibitor ouabain (half-maximal inhibitory concentration [IC<sub>50</sub>] ~100 μM; Price and Lingrel, 1988) than its human α1 orthologue (IC<sub>50</sub> 5–50 nM; Crambert et al., 2000) due to the RD substitutions (i.e., Q118R/N129D for human α1 pumps). RD mutations are commonly used for oocyte Na/K pump recordings (Hilbers et al., 2016; Stanley et al., 2016; Yaragatupalli et al., 2009) to allow for separation of exogenous and endogenous pump signals based on sensitivity to the inhibitor. However, given that RD mutations alter ion binding reactions (Vedovato and Gadsby, 2010), we chose not to introduce RD mutations into the human α1 isoform because the effects of FXYPs on ion apparent affinities were expected to be small. For kinetic analysis, we considered only experiments with Na/K pump currents at least sixfold above the maximal endogenous Na/K pump current of uninjected oocytes (i.e., ≥150 nA in TEVC; ≥3.5 pA in patch), which is 25 nA with 90 mM external Na<sup>+</sup> (Stanley et al., 2015); 14 ± 8 nA at 145.5 mM Na<sup>+</sup> + 4.5 K<sup>+</sup> (n = 26, four batches of oocytes) in TEVC; or 0.55 pA in patches (Meyer et al., 2017). This ensures negligible contribution from endogenous pumps.

## Electrophysiology

TEVC was performed 3–6 d after cRNA injection using an OC-725C amplifier (Warner Instruments) or a CA-1B amplifier (Dagan) controlled by pClamp software (Molecular Devices). Only FXYD1 experiments and its cotemporaneous controls were performed using the CA-1B. After completing the experiments, we noticed that the voltage dependence of  $\alpha 1\beta 1$  results with the CA-1B differed from those with the OC-725C. These differences were the result of an error in the output gain of the digidata controlling the CA-1B, requiring a nonconventional 14.5 mV/V gain instead of the conventional 20 mV/V. The voltage values were corrected offline, and the steady-state curves for  $\alpha 1\beta 1$  obtained on either amplifier were indistinguishable from each other (e.g., see Table 2). All currents were digitized at 10 kHz with a Digidata 1440 A/D converter and continuously recorded with a Minidigi 1A at 1 kHz (both AD converters from Molecular Devices). Current and voltage glass electrodes had 0.2–1 M $\Omega$  of resistance (filled with 3 M KCl).

Before recording, oocytes were incubated for 30 min in a Na<sup>+</sup>-loading solution containing (in mM) 90 NaOH, 20 tetraethylammonium-OH, 40 HEPES, and 0.2 EGTA, titrated to pH 7.2 with sulfamic acid (~220 mOsm/kg), and then kept until recording in a 125 mM Na<sup>+</sup><sub>o</sub> solution containing (in mM) 133 methanesulfonic acid (MS), 5 Ba(OH)<sub>2</sub>, 1 Mg(OH)<sub>2</sub>, 0.5 Ca(OH)<sub>2</sub>, 10 HEPES, and 125 NaOH, titrated to pH 7.6 with MS (~260 mOsm/kg). Upon clamping, the oocytes were perfused with a Na<sup>+</sup><sub>o</sub> solution (~300 mOsm/kg) that contained (in mM) 150 NaOH, 5 BaCl<sub>2</sub>, 1 MgCl<sub>2</sub>, 0.5 CaCl<sub>2</sub>, and 5 HEPES, titrated to pH 7.4 with MS. K<sup>+</sup><sub>o</sub> was added by mixing the Na<sup>+</sup><sub>o</sub> solution with a solution in which 150 mM KOH replaced 150 mM NaOH. Ouabain was directly dissolved in external solutions.

Inside-out patch clamp was performed as previously described (Meyer et al., 2017), on the animal pole of manually devitellinized oocytes, using a 3900A amplifier (Dagan) controlled by pClamp and digitized with a Digidata 1550A A/D converter (Molecular Devices). Current was continuously monitored with a Minidigi 1B at 100 Hz. The borosilicate pipettes were fire polished to  $\geq 15$ - $\mu$ m diameter and coated with sylgard. Pipette resistance was 0.5–0.7 M $\Omega$  when filled with pipette (extracellular) solution containing (in mM) 140 NMDG, 5 KCl, 5 BaCl<sub>2</sub>, 1 MgCl<sub>2</sub>, 0.5 CaCl<sub>2</sub>, and 5 HEPES, titrated to pH 7.4 with HCl (~280 mOsm/kg). The patch was formed in a bath solution containing (in mM) 100 KOH, 20 KCl, 10 HEPES, 4 MgCl<sub>2</sub>, and 2 EGTA, titrated to pH 7.0 with L-aspartic acid (~240 mOsm/kg), and the solution was switched to the recording solution after excision. This recording intracellular solution was made by mixing solutions containing (in mM) 1 MgCl<sub>2</sub>, 10 tetraethylammonium-Cl, 10 HEPES, and 5 EGTA, and either 140 NaOH, 140 NMDG, or 140 KOH (pH 7.4 with L-glutamic acid; ~280 mOsm/kg). After mixing to obtain the various intracellular Na<sup>+</sup> (Na<sup>+</sup><sub>i</sub>) concentrations, solutions were degassed for 5–10 min in a vacuum desiccator. Solution exchange was achieved with a piezo solution switcher (Siskiyou). Just before recording, MgATP (A9187; Sigma-Aldrich) was added to the internal solutions from 200 mM stocks (in filtered double distilled H<sub>2</sub>O, pH 7.2 with NMDG<sup>+</sup>, kept at –20°C). PKA catalytic subunit (prepared weekly as 50 mg/ml stocks in 6 mg/ml

dithiothreitol, according to manufacturer's instructions; P2645; Sigma-Aldrich) was also added to the internal solution at a final concentration of ~5  $\mu$ M just before recording.

## Western blotting

Plasma membrane preparations were performed with 14–40 oocytes 3–5 d after injection with the indicated cRNA combinations. Oocytes were homogenized in oocyte homogenization buffer (OHB; 250 mM sucrose, 5 mM MgCl<sub>2</sub>, 10 mM HEPES, 1 mM PMSF, and protease inhibitor cocktail were added before starting, pH 7.4) in a glass Dounce homogenizer on ice. The homogenate was centrifuged at 500 g for 10 min at 4°C to remove cellular debris. The supernatant was kept on ice, and the procedure was repeated with the pellets. The two supernatants were combined and laid on top of two layers (4.5 ml each) of OHB + 20% sucrose and OHB + 50% sucrose and centrifuged at 30,000 g for 1 h at 4°C in a swinging bucket rotor (Sw41Ti). After centrifugation, two major membrane bands were visible. Both the light (within 20% sucrose layer) and heavy (at 20–50% interface) bands were collected and diluted twofold with OHB. The membranes were pelleted at 100,000 g at 4°C for 30 min.

The same total protein amount from each injection condition (quantified by BCA Protein Assay Kit; Thermo Fisher Scientific) was mixed with equal volumes of Laemmli sample buffer (Sigma-Aldrich; 4% SDS, 20% glycerol, 10% 2-mercaptoethanol, 0.004% bromphenol blue, and 0.125 M Tris HCl, pH 6.8) and 8 M urea. The mix was loaded into a 4–20% polyacrylamide gel (4–20% Mini-Protean TGX Precast Protein Gels; Bio-Rad). After electrophoresis, proteins were transferred onto polyvinylidene difluoride membranes by electroblotting in 25 mM Tris, 192 mM glycine, and 20% methanol (pH 8.0) for 3 h at a constant current of 30 mA. Polyvinylidene difluoride membranes were blocked with milk for 1 h at room temperature, followed by overnight incubation at 4°C with 1:5,000 dilutions of mouse anti-Na/K pump  $\alpha$ -subunit antibody a5 (Developmental Studies Hybridoma Bank) or 1:5,000 rabbit anti-FXYD1/PLM antibody (ab76597, Abcam). After three washes with PBS containing 0.1% Tween-20 (vol/vol), the membranes were incubated with 1:20,000 dilutions of secondary antibodies IRDye 800CW goat anti-mouse or IRDye 680RD goat anti-rabbit (LI-COR) for 1 h at room temperature. Finally, the membranes were washed three times with PBS + 0.1% Tween-20 and visualized via Infrared Fluorescence Odyssey Imagen System (LI-COR).

## Imaging

Five oocytes in each condition (injected with  $\alpha 1\beta 1$ ,  $\alpha 1\beta 1$ FXYD1, or  $\alpha 1\beta 1$ FXYD6 and uninjected with or without preincubation with 10  $\mu$ M unlabeled ouabain) were incubated for 15 min with 1  $\mu$ M BODIPY FL-ouabain (Thermo Fisher Scientific), followed by three rinses in 125 mM Na<sup>+</sup> external solution. Immediately after rinsing, oocytes from two different batches were imaged on a Nikon Ti-E Microscope in the Texas Tech University Health Sciences Center's Image Analysis Core Facility, using the Alexa Fluor 488 excitation/emission filter set, with a 10 $\times$  objective. The confocal plane was placed as close to the equator as possible (sometimes the equator exceeded the maximum image field). The images were analyzed by measuring the total fluorescence



intensity in two concentric circles and then subtracting the intensity in the inner circle from the intensity in the external circle that contained the plasma membrane.

### PKA and PKA inhibitor (PKI) injections

For some  $\alpha 1\beta 1$  or  $\alpha 1\beta 1\text{FX}1\text{YD}1$  TEVC experiments, oocytes were injected with PKA or the PKI fragment 6–22 amide (P6062; Sigma-Aldrich) before recording. These oocytes were  $\text{Na}^+$ -loaded for 30 min (as above), kept in  $\text{Na}^+$  solution for 30 min, injected with PKA ( $\sim 2 \mu\text{M}$ , V5161; Promega) or PKI ( $\sim 250 \mu\text{M}$ ), and kept in  $\text{Na}^+$  solution for  $\geq 45$  min until recording. Oocyte volume was assumed to be  $1 \mu\text{l}$  (typical oocyte diameter is  $\sim 1 \text{ mm}$ ; Dascal, 2000).

### Data analysis

Electrophysiological data were analyzed using software from pClamp (Molecular Devices) and Origin (OriginLab). The  $K_{0.5}$  for  $\text{K}^+$  or for  $\text{Na}^+$  was determined by fitting the Hill equation,

$$I = I_{\max} \left[ \frac{(\text{ion})^H}{K_{0.5}^H + (\text{ion})^H} \right],$$

to the  $[\text{K}^+]_o$  dependence of ouabain-sensitive currents (for  $K_{0.5, \text{K}^+}$ ) or the  $[\text{Na}^+]_i$ -dependence of ATP-activated currents (for  $K_{0.5, \text{Na}^+}$ ), where the maximal pump current ( $I_{\max}$ ) is the current stimulated by infinite (ion);  $K_{0.5}$  is the (ion) at which  $I = I_{\max}/2$ ; and  $H$  is the Hill coefficient, which was fixed at 1.6 for fits to external  $\text{K}^+$ -dependent curves (Jaisser et al., 1994). Ouabain-sensitive transient currents were integrated, and the time dependence of charge was fitted (performing the fit in the integral instead of the current improves detection of the slow component), starting 3 ms after turning on the pulse, to a mono-exponential equation extrapolated to the beginning of the pulse,

$$Q = Q_s e^{(-t/\tau)} + C,$$

where  $Q_s$  is the charge moved in the slow component,  $\tau$  is the relaxation time constant, and  $C$  is a constant that includes the charge moved in the fast component (before 3 ms). We use the ratio  $Q_s/Q$  at +40 mV in steady state to calculate the fraction of the charge in the slow component.

Ouabain-sensitive charge-voltage (Q-V) curves (from the steady-state value of the current integrals) were fitted with the Boltzmann equation,

$$Q = Q_{\text{hyp}} - \frac{Q_{\text{tot}}}{1 + \exp \left[ \frac{z_q e (V - V_{0.5})}{kT} \right]},$$

where  $Q_{\text{hyp}}$  is the charge moved by hyperpolarizing voltage changes,  $Q_{\text{tot}}$  is the total charge moved,  $V_{0.5}$  is the voltage at the center of the distribution,  $z_q$  is the apparent valence of a charge crossing the whole electric field,  $e$  is the elementary charge,  $k$  is the Boltzmann constant, and  $T$  is temperature (in Kelvin). The slope factor is  $kT/ez_q$ . The Q-V curves were normalized by subtracting  $Q_{\text{hyp}}$  from the  $Q$  moved at each voltage and dividing by  $Q_{\text{tot}}$ .

The turnover rate of pump activity was calculated as

$$\text{Turnover} = I_P / Q_{\text{tot}},$$

where  $I_P$  is the pump current and  $Q_{\text{tot}}$  is the total charge calculated from a Boltzmann fit to the Q-V curve. As the charge moved by each individual pump during the  $\text{E1P}(3\text{Na}^+) \leftrightarrow \text{E2P}$  transition (presumably one elementary charge; Nakao and Gadsby, 1986) is constant,  $Q_{\text{tot}}$  is an estimate of the number of functional pumps at the plasma membrane.

### Online supplemental material

Fig. S1 shows kinase activity of the same PKA batch used in Na/K pump experiments, in a patch from an oocyte expressing cystic fibrosis transmembrane conductance regulator (CFTR) channels.

## Results

### FX1YD subunits alter interaction with $\text{K}^+$ .

Experiments were designed to determine the effects of human FX1YD subunit isoforms on the human  $\alpha 1\beta 1$  pump's interaction with external  $\text{K}^+$  ( $\text{K}^+_o$ ). Fig. 2 illustrates the analysis of a dose response for  $\text{K}^+_o$ -induced current with a  $\text{Na}^+$ -loaded oocyte 5 d after injection with an  $\alpha 1\beta 1$  cRNA mixture (without FX1YDs). The continuous recording from an oocyte held at  $-50$  mV and bathed in mammalian-like cation solutions (Fig. 2 A;  $[\text{Na}^+]_o + [\text{K}^+]_o = 150$  mM) shows that application of  $10$  mM  $\text{K}^+_o$  (i.e.,  $140$  mM  $\text{Na}^+_o + 10$  mM  $\text{K}^+_o$ ) induced a large outward current (due to the extrusion of one net positive charge per cycle) that decreased with stepwise reductions of  $\text{K}^+_o$  concentration. A brief application of  $0.5$  mM ouabain inhibited (irreversibly within the experimental duration) all  $\text{K}^+_o$ -induced outward current by subsequent applications of  $\text{K}^+_o$ , demonstrating robust overexpression of exogenous human pumps. Vertical current deflections along the recording indicate application of  $100$ -ms-long square pulse to voltages between  $-100$  and  $+40$  mV to obtain current-voltage (I-V) plots of ouabain-sensitive currents (Fig. 2 B, current before ouabain minus the current after ouabain application in the same external condition). Hill equations were fitted to the  $\text{K}^+_o$  concentration dependence of ouabain-sensitive currents at each voltage (Fig. 2 C) to determine the  $K_{0.5}$  for  $\text{K}^+_o$ , which was then plotted against voltage (Fig. 2 D).  $K_{0.5, \text{K}^+}$  was determined in oocytes coinjected with  $\alpha 1\beta 1$  and FX1YD1, FX1YD2, FX1YD4, FX1YD6, or FX1YD7. Table 1 summarizes the small effect of FX1YD isoforms on the mean  $K_{0.5}$  values at  $-100$  and  $0$  mV; FX1YD1, FX1YD4, and FX1YD7 increased  $K_{0.5}$ , at both voltages, with FX1YD4 and FX1YD7 showing larger effects at negative voltages, FX1YD2 reduced  $K_{0.5}$  at negative voltages, and FX1YD6 increased  $K_{0.5}$  at  $0$  mV. In contrast to the large currents ( $>150$  nA at  $-50$  mV) in oocytes expressing  $\alpha 1\beta 1$  with FX1YD $_x$ ,  $4.5$  mM  $\text{K}^+_o$  induced only  $14 \pm 8$  nA ( $n = 26$ ) in four batches of uninjected oocytes,  $11 \pm 3$  nA ( $n = 8$ ) in two batches of FX1YD1-alone-injected oocytes, and  $8 \pm 3$  nA ( $n = 5$ ) in one batch of FX1YD6-alone-injected oocytes. This ensures that the signals we evaluated come from human  $\alpha 1\beta 1$ -expressing oocytes, without contamination from endogenous pumps. Our results with human isoforms resemble previously reported effects with FX1YD isoforms and  $\alpha 1\beta 1$  isozymes of diverse origin (Béguin et al., 1997, 2001, 2002; Bossuyt et al., 2009; Crambert

et al., 2002; Delprat et al., 2007; Geering, 2006; Li et al., 2005; Lindzen et al., 2003a), but the amplitude of changes in  $K_{0.5}$  we observed appear to be smaller in magnitude.

#### FXYP subunits alter interaction with $\text{Na}^+$

To determine the effect of each FXYP isoform on the interaction of  $\alpha 1\beta 1$  with extracellular  $\text{Na}^+$  ( $\text{Na}^+_{\text{o}}$ ) we measured transient currents of  $\text{Na}^+$ -loaded oocytes bathed in 150 mM  $\text{Na}^+_{\text{o}}$ , without  $\text{K}^+_{\text{o}}$  (Fig. 3), a condition in which the pump is restricted to its phosphorylated partial reactions. Square voltage pulses evoke transient currents that reflect either  $\text{Na}^+_{\text{o}}$  binding and occlusion (hyperpolarizing pulse) or deocclusion and unbinding (depolarizing pulse) events that are rate-limited by the pump's transitions between  $\text{E1P}(3\text{Na}^+)$  and  $\text{E2P}$  states (Fig. 1 B, dotted box). A pulse protocol is applied first without and then with ouabain to inhibit the currents owing to  $\text{Na}/\text{K}$ -pump conformational changes. Representative ouabain-sensitive transient currents (currents in  $\text{Na}^+_{\text{o}}$  minus the currents in  $\text{Na}^+_{\text{o}}$  with ouabain) from oocytes expressing  $\alpha 1\beta 1$  alone (Fig. 3 A) or coexpressed with FXYP1 (Fig. 3 B), FXYP2b (Fig. 3 C), FXYP4 (Fig. 3 D), FXYP6 (Fig. 3 E), or FXYP7 (Fig. 3 F) illustrate the unique effect of each FXYP isoform on transient currents.

The multiexponential relaxation rates of the transient current during each voltage step reflect the rates of partial reactions during the pump's  $\text{Na}^+$  translocation steps; the slowest component of the relaxation rate represents the  $\text{Na}^+$  reocclusion/deocclusion reaction (Castillo et al., 2011; Holmgren et al., 2000; Moreno et al., 2020). The fastest components (corresponding to the reaction  $\text{E2P}(2\text{Na}^+) \leftrightarrow \text{E2P} + 2\text{Na}^+_{\text{o}}$ , Fig. 1 B) cannot be time resolved with the TEVC technique, whereas the slow component ( $\text{E1P}(3\text{Na}^+) \leftrightarrow \text{E2P}(2\text{Na}^+) + \text{Na}^+_{\text{o}}$ ; Fig. 1 B) can be resolved easily. Assuming that the maximal relaxation rate at extreme negative voltages is not changed, the shift in the voltage dependence (Fig. 4 A) of relaxation rates,  $1/\tau$  from a monoexponential fitted to the current integral (similar to the dashed lines representing

Table 1. Mean  $K_{0.5}$  and  $I_{\text{max}}$  from  $[\text{K}^+_{\text{o}}]$  dependence

Condition	$K_{0.5}$ for $\text{K}^+_{\text{o}}$ (mM)		$I_{\text{max}}$ (nA)	n
	-100 mV	0 mV	$\geq 150$ nA, 0mV	
$\alpha 1\beta 1$	$1.6 \pm 0.3$	$0.9 \pm 0.2$	$365 \pm 144$	24
FXYP1	$2.0 \pm 0.4^{**}$	$1.2 \pm 0.2^{**}$	$275 \pm 110$	32
FXYP2	$1.0 \pm 0.3^{**}$	$1.0 \pm 0.3$	$290 \pm 43$	8
FXYP4	$2.8 \pm 0.6^{**}$	$1.5 \pm 0.1^{**}$	$330 \pm 117$	8
FXYP6	$1.4 \pm 0.2$	$1.2 \pm 0.2^{**}$	$340 \pm 66$	11
FXYP7	$2.4 \pm 0.3^{**}$	$1.4 \pm 0.2^{**}$	$278 \pm 86$	9

Mean  $K_{0.5}$  values at -100 mV and 0 mV. Errors represent SD; n is the number of experiments. \*\*, Significantly different with respect to  $\alpha 1\beta 1$  alone by t test:  $P < 0.001$ .

fits to the currents in Fig. 3), indicate that  $\text{Na}^+_{\text{o}}$  reocclusion was slowed by FXYP1, FXYP6, and FXYP2, and probably unaltered by FXYP7.

From the ouabain-sensitive transient current traces in Fig. 3, it is also clear that the amplitude of each multiexponential component of transient current induced by the pulse to +40 mV is altered by all five FXYP proteins. Compared with  $\alpha 1\beta 1$  alone, the ratio of charge moved in the slow component divided by the steady-state charge from the current integral ( $Q_s/Q$ ) was reduced significantly by FXYP1, FXYP2, and FXYP6 but increased by FXYP4 and FXYP7. These changes to the rate and proportion of the slow transient provide insight into the mechanism of action of these FXYPs (see Discussion).

Relative changes in apparent affinity for  $\text{Na}^+_{\text{o}}$  can be estimated from the shift of the voltage dependence of the steady-state charge distribution (Fig. 4 B). The transient current elicited by each voltage pulse, measured when the pulse was turned off, was integrated, and the resulting charge was plotted as a

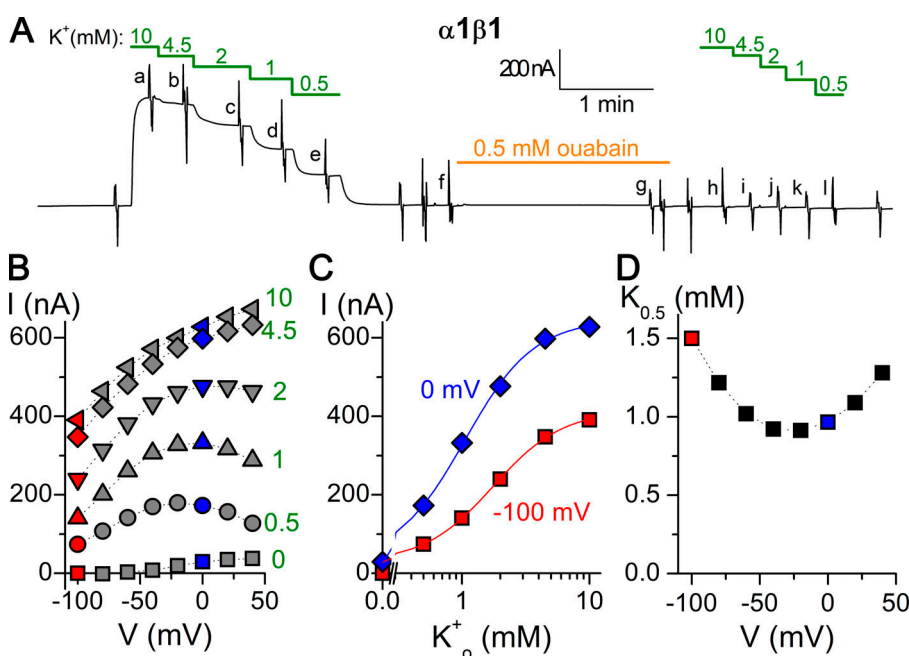
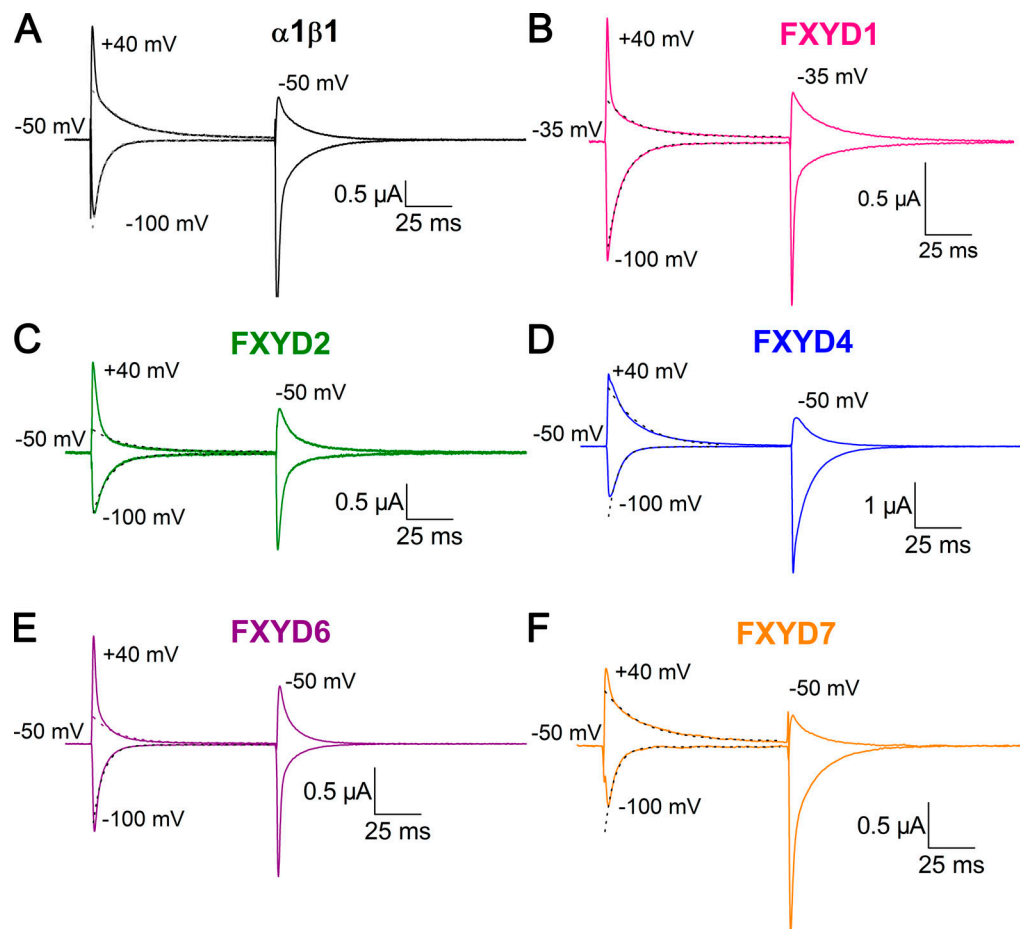


Figure 2. Recording and analysis of an experiment to determine the  $K_{0.5}$  for  $\text{K}^+_{\text{o}}$ . (A) Current at -50 mV of a  $\text{Na}^+$ -loaded oocyte overexpressing the  $\alpha 1\beta 1$  pump, bathed in  $\text{Na}^+_{\text{o}}$  solution. Substituting  $\text{Na}^+_{\text{o}}$  with  $\text{K}^+_{\text{o}}$  stimulated outward current in a  $[\text{K}^+_{\text{o}}]$ -dependent manner. Application of 0.5 mM ouabain for 2 min blocked currents in subsequent  $\text{K}^+$  applications. Vertical deflections along the recording indicate pulses to voltages between -100 and +40 mV. Lowercase letters indicate currents used to obtain ouabain-sensitive currents in B. (B) I-V plot of ouabain-sensitive current (current before ouabain application in the same condition) measured during the last 5 ms of 100-ms-long voltage pulses. (C)  $[\text{K}^+_{\text{o}}]$  dependence of ouabain-sensitive current at -100 and 0 mV fitted with Hill equations (line plots). (D) Voltage dependence of  $K_{0.5}$  for  $\text{K}^+_{\text{o}}$ .



**Figure 3. Effect of FXYP subunits on transient currents.** (A–F) Ouabain-sensitive currents elicited by voltage steps from the holding potential to  $-100$  and  $+40$  mV recorded from oocytes bathed in external  $\text{Na}^+$  solution 3–6 d after injection with  $\alpha 1\beta 1$  (A),  $\alpha 1\beta 1\text{FXYP1}$  (B),  $\alpha 1\beta 1\text{FXYP2}$  (C),  $\alpha 1\beta 1\text{FXYP4}$  (D),  $\alpha 1\beta 1\text{FXYP6}$  (E), or  $\alpha 1\beta 1\text{FXYP7}$  (F). The oocyte in B was held at  $-35$  mV, and the rest were held at  $-50$  mV. Depolarizing voltage pulses from the holding potential produce transient outward currents, whereas hyperpolarizing voltage pulses produce transient inward currents. The dashed lines are monoexponential fits to the current, beginning 3 ms after the voltage step.

function of the applied voltage (Q–V curve). A Boltzmann equation was fitted to the data from each individual experiment (see Materials and methods), giving the total charge ( $Q_{\text{tot}}$ ), slope factor ( $kT/z_e e$ ), and midpoint voltage ( $V_{0.5}$ ), which are summarized in Table 2.

A positive shift of the  $V_{0.5}$  indicates an increase, while a negative shift indicates a decrease, of the apparent affinity for  $\text{Na}^+$  (approximately twofold change in apparent affinity per  $\sim 25$ -mV shift; Holmgren and Rakowski, 2006). Therefore, our results indicate that the apparent affinity for  $\text{Na}^+$  is reduced (1.5–2-fold) by FXYP1, FXYP2, and FXYP6 and increased ( $\sim 2$ -fold) by FXYP4 and FXYP7 (Fig. 4 B and Table 2). It should be noted that this apparent affinity links direct effects on ion binding with effects on the E1P/E2P equilibrium.

Given that FXYP6 accelerates the  $\text{Na}^+$  deocclusion rate (i.e., the rates measured at positive potentials in Fig. 4 A), which, together with deocclusion of  $2 \text{ K}^+$  toward the intracellular side, is one of the rate-limiting steps in the cycle, we calculated the turnover rate of  $\text{Na}^+/\text{K}^+$  transport at physiological  $\text{K}^+$  (Fig. 5) by dividing the pump activity (pump current) by the number of pumps in the plasma membrane (which is directly proportional

to the total charge; see Materials and methods). FXYP6 increased the turnover rate by 30–50% (depending on voltage), probably reflecting the increased rate of the  $\text{E1P}(3\text{Na}^+) \rightarrow \text{E2P}$  transition described above. The turnover rates observed with the other FXYP isoforms nearly overlapped with  $\alpha 1\beta 1$  alone, although FXYP4 and FXYP7 seemed to reduce the turnover rate at negative voltages ( $\sim 25\%$  at  $-80$  mV, probably owing to a strong voltage-dependent inhibition by  $\text{Na}^+$ ), while FXYP1 induced a small ( $\sim 15\%$ ), but statistically significant ( $P < 0.05$ ), reduction of the turnover rate at 0 mV, from  $14.9 \pm 3.0$  ( $n = 47$ ) in  $\alpha 1\beta 1$  to  $12.9 \pm 3.0 \text{ s}^{-1}$  ( $n = 20$ ) in  $\alpha 1\beta 1\text{FXYP1}$ , consistent with a  $\sim 25\%$  reduction previously reported in studies with purified protein (Mishra et al., 2015).

#### FXYP1 and FXYP6 reduce surface expression of $\alpha 1\beta 1$

After a long struggle to achieve consistently high expression levels for kinetic measurements in oocytes injected with either FXYP1 or FXYP6, we noticed that these isoforms substantially reduced the total number of functional pumps in the membrane (i.e., they reduced total charge and  $\text{Na}/\text{K}$  pump current). Retrospectively and prospectively, we compared the amplitude of

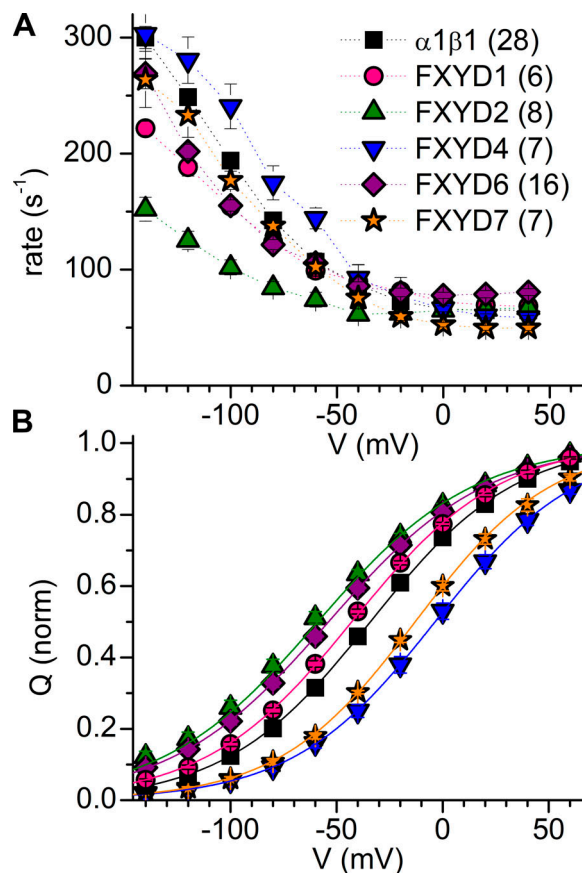


Figure 4. **Effect of FXYDs on charge movement.** (A) Mean transient charge-movement rate for  $\alpha 1\beta 1$  alone or coexpressed with FXYD proteins. The rates were calculated from monoexponential fits to the integral of transient currents. (B) Mean normalized Q-V curves for  $\alpha 1\beta 1$  alone or when coexpressed with FXYD isoforms. Error bars are SEM in both panels. See also Table 2 (note that the  $\alpha 1\beta 1$  and  $\alpha 1\beta 1$ FXFYD1 shown here are those that started at a holding potential of  $-50$  mV).

Na/K pump current in oocytes injected with  $\alpha 1\beta 1$  alone with that in oocytes injected with  $\alpha 1\beta 1$ FXFYD1 or  $\alpha 1\beta 1$ FXFYD6 (Fig. 6). On average, pump currents from oocytes expressing FXFYD1 (Fig. 6 A) and FXFYD6 (Fig. 6 B) were reduced to  $52\% \pm 23\%$  ( $n = 45$ ) and  $30\% \pm 20\%$  ( $n = 29$ ), respectively, of the current from oocytes expressing  $\alpha 1\beta 1$  alone. This analysis includes oocytes grouped by oocyte batch (seven batches for each FXFYD), measured in a 2-d span (Many of these oocytes did not reach our 150-nA  $K^+$ -induced current threshold for the kinetic analysis in previous figures). In addition to the strong reduction in functional expression, FXFYD6 also increased oocyte death rate following the third day after injection, largely complicating the measurements.

To test if the changes in functional expression are due to a reduced number of Na/K pump molecules at the plasma membrane or to another form of inhibition of the pumps remaining there, we used two semiquantitative methods: labeling with BODIPY FL-ouabain and Western blot of plasma membrane preparations (Fig. 7). Five different oocyte groups were labeled by a 15-min incubation in BODIPY FL-ouabain; representative confocal images (Fig. 7 A) illustrate that  $\alpha 1\beta 1$ -injected oocytes display larger fluorescence than oocytes injected with

$\alpha 1\beta 1$ FXFYD1 or  $\alpha 1\beta 1$ FXFYD6. Uninjected oocytes showed lower intensity than all injected oocytes, but larger intensity than uninjected oocytes preincubated in unlabeled ouabain, demonstrating specificity of the signal. The bar graph below the images plots the average fluorescence intensity at the plasma membrane in two batches of oocytes, normalized to the intensity in  $\alpha 1\beta 1$ -injected oocytes. A representative Western blot probed with an  $\alpha$ -specific antibody (Fig. 7 B) shows that plasma membranes from oocytes injected with  $\alpha 1\beta 1$  (lane 2) have more  $\alpha 1$  protein than membranes from oocytes injected with  $\alpha 1\beta 1$ FXFYD1 (lane 3), which clearly has more  $\alpha 1$  than oocytes injected with FXFYD alone (lane 4). The bar graph plots the mean average from five membrane preparations from four batches of oocytes (Fig. 7 B). Survival of oocytes injected with  $\alpha 1\beta 1$ FXFYD6 was too low to make the membrane preparations.

#### PKA restores functional expression of FXFYD1 pumps

FXFYD1's intracellular C-terminal region is rich in serine and threonine residues, many of which are phosphorylated by protein kinases (Palmer et al., 1991). We evaluated the effects of PKA on Na/K pump currents under TEVC (Fig. 8). To avoid confounding effects due to plausible phosphorylation by the relatively active endogenous PKA (Artigas et al., 2006), we performed control experiments on oocytes with PKI. TEVC experiments were performed intercalating measurements in PKA- and PKI-injected oocyte groups, on the same day, using the same setup, with the same solutions, and by the same experimentalist.

Representative currents from oocytes expressing  $\alpha 1\beta 1$ FXFYD1  $\sim 4.5$  h after injection with PKA (Fig. 8 A) or PKI (Fig. 8 B) illustrate dose-dependent effects for  $K^+$  at the holding potential ( $-35$  mV). At all voltages, the  $K_{0.5,K^+}$  for PKA-injected oocytes overlap with PKI-injected ones (Fig. 8 C), meaning that PKA did not reverse the small change in affinity induced by FXFYD1, consistent with a previous report (Bibert et al., 2008). However, it is evident that the oocytes in Fig. 8, A and B, produce different current levels. The mean 10 mM  $K^+$ -induced current measured in two batches of oocytes show that  $\alpha 1\beta 1$ FXFYD1-expressing oocytes injected with PKA have larger outward currents than those injected with PKI, an effect that is absent in oocytes expressing  $\alpha 1\beta 1$  alone (Fig. 8 D). Upon normalization to the value measured in PKA-injected oocytes on the same day, the mean current for  $\alpha 1\beta 1$ FXFYD1 was  $1 \pm 0.21$  ( $n = 11$ ) in PKA-injected oocytes and  $0.54 \pm 0.19$  ( $n = 10$ ) in PKI-injected ones, while the mean currents for  $\alpha 1\beta 1$  alone were  $1 \pm 0.35$  ( $n = 12$ ) and  $0.88 \pm 0.23$ . Oocytes expressing  $\alpha 1\beta 1$ FXFYD1 also showed proportionally larger total charge ( $Q_{tot}$ ) when injected with PKA compared with those injected with PKI. Therefore, the turnover rate remained nearly constant between PKA- and PKI-injected oocytes (Fig. 8 E). The apparent affinity for  $Na^+$  of  $\alpha 1\beta 1$ FXFYD1 was unaffected by PKA, as the center for the Boltzmann distribution of Q-V curves was  $-39.2 \pm 4.4$  mV ( $n = 20$ ) for PKA-injected and  $-39.1 \pm 7.4$  ( $n = 26$ ) for PKI-injected oocytes expressing  $\alpha 1\beta 1$ FXFYD1.

#### Effect of FXYDs on interaction with $Na^+$

Most FXFYD isoforms have been shown to modulate the apparent affinity for  $Na^+$ . We evaluated  $Na^+$  interaction by measuring the  $Na^+$  concentration dependence of ATP-activated currents in



Table 2. Transient charge movement parameters

Condition	Rate <sub>-100</sub> (s <sup>-1</sup> )	Rate <sub>+40</sub> (s <sup>-1</sup> )	V <sub>0.5</sub> (mV)	Q <sub>tot</sub> (nC)	kT/z <sub>q</sub> e (mV)	Q <sub>s</sub> /Q (%)	n
α1β1	194 ± 21	65 ± 9	-34 ± 5	17 ± 8	34 ± 2	72 ± 6	28
FXYD1	154 ± 14**	68 ± 6	-43 ± 2**	11 ± 3	34 ± 2	66 ± 4*	6
FXYD2	102 ± 19**	67 ± 13	-61 ± 9**	20 ± 8	39 ± 3	59 ± 2**	8
FXYD4	251 ± 51**	59 ± 5	-4 ± 9**	18 ± 13	33 ± 1	78 ± 3*	7
FXYD6	155 ± 19**	80 ± 12**	-54 ± 7**	16 ± 3	37 ± 3	58 ± 4**	16
FXYD7	167 ± 21*	49 ± 6**	-13 ± 4**	16 ± 6	32 ± 4	78 ± 5*	7
α1β1 <sub>-35 mV</sub>	156 ± 20	54 ± 4	-30 ± 4	26 ± 7	29 ± 2	77 ± 7	13
FXYD1 <sub>-35 mV</sub>	120 ± 21**	54 ± 9	-40 ± 7**	18 ± 7	31 ± 2	68 ± 6**	26

Some FXYD1 experiments and some α1β1 controls started from a holding potential of -35 mV in the Dagan amplifier and are shown separately. Errors represent SD; n is the number of determinations. Q<sub>tot</sub> was determined from the Boltzmann fits to Q-V in individual oocytes (Materials and methods). Q<sub>s</sub>/Q is the charge of the slow component divided by the steady-state value from the transient-current integral in pulses to +40 mV. Significantly different with respect to α1β1 alone by t test: \*P < 0.05; \*\*, P < 0.001.

large inside-out patches, allowing for rapid and precise exchange of internal ion composition, while the pipette extracellular solution remained constant and contained NMDG<sup>+</sup> with saturating 5 mM K<sup>+</sup><sub>o</sub> (Figs. 9 and 10 and Table 3). When measurements were performed with a mixture of NMDG<sup>+</sup><sub>i</sub> and Na<sup>+</sup><sub>i</sub> (without intracellular K<sup>+</sup> [K<sup>+</sup><sub>i</sub>]), the K<sub>0.5</sub> observed with each FXYD protein was not significantly different from α1β1 alone (P ≤ 0.05; Fig. 9 and Table 3). The continuous trace (Fig. 9 A)

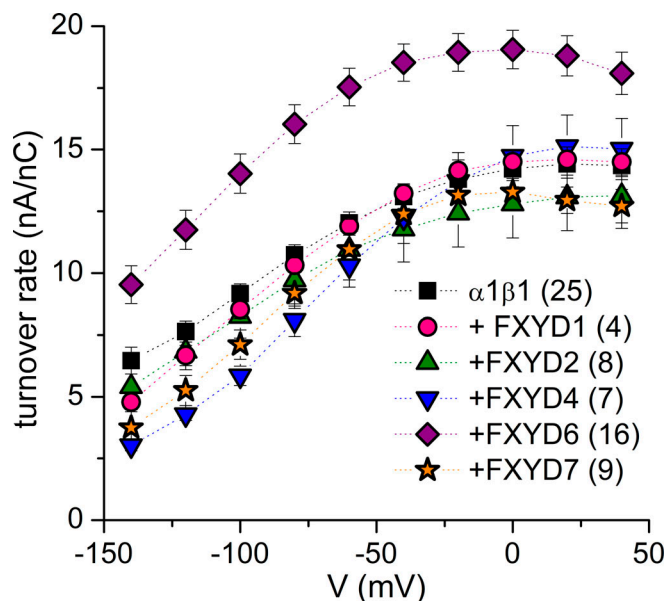


Figure 5. **Effect of FXYD isoforms on turnover rate.** Mean turnover rate at 4.5 mM K<sup>+</sup><sub>o</sub> as a function of voltage. Error bars are SEM. Data from Warner amplifier are shown. Values at 0 mV are (± SD in s<sup>-1</sup>): 14.9 ± 3.0 (n = 47, data from Warner and Dagan amplifiers) for α1β1, 12.9 ± 3.0\* for α1β1FXYD1 (n = 20, data from Warner and Dagan amplifiers), 12.8 ± 3.9 for α1β1FXYD2, 14.7 ± 3.3 for α1β1FXYD4, 19.1 ± 3.1 for α1β1FXYD6\*\*, and 13.3 ± 1.7 for α1β1FXYD7. Note that there are more oocytes where we measured pump current at 4.5 mM K<sup>+</sup><sub>o</sub> and charge movement than full dose-response curves and charge movement. Significantly different with respect to α1β1 alone by t test: \*, P < 0.05; \*\*, P < 0.001.

shows a typical experiment in a patch excised from an oocyte expressing α1β1 alone. We first applied 25 mM Na<sup>+</sup><sub>i</sub> and then added a saturating concentration of MgATP (4 mM), reversibly activating Na/K pump current. The first activation is biphasic, with a nearly instantaneous phase (rate limited by solution exchange) and a slow phase that develops in tens of seconds. The slow fraction was reduced when MgATP was reapplied in 5, 2, and 1 and again in 25 mM Na<sup>+</sup>, similar to previous reports in giant patches excised from rat ventricular myocytes (Friedrich et al., 1996; Hilgemann, 1997). However, although generally reduced in subsequent applications, the initial amplitude of this slow component was variable (see Discussion). At steady state, the ATP-induced current amplitude depended on the Na<sup>+</sup><sub>i</sub> concentration, as shown in the normalized dose-response curves for

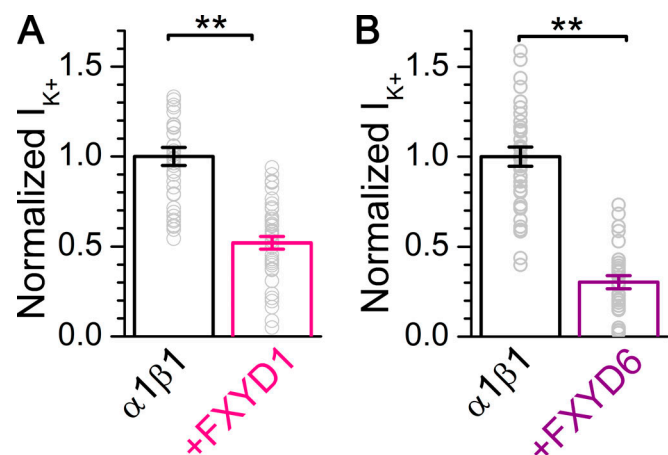
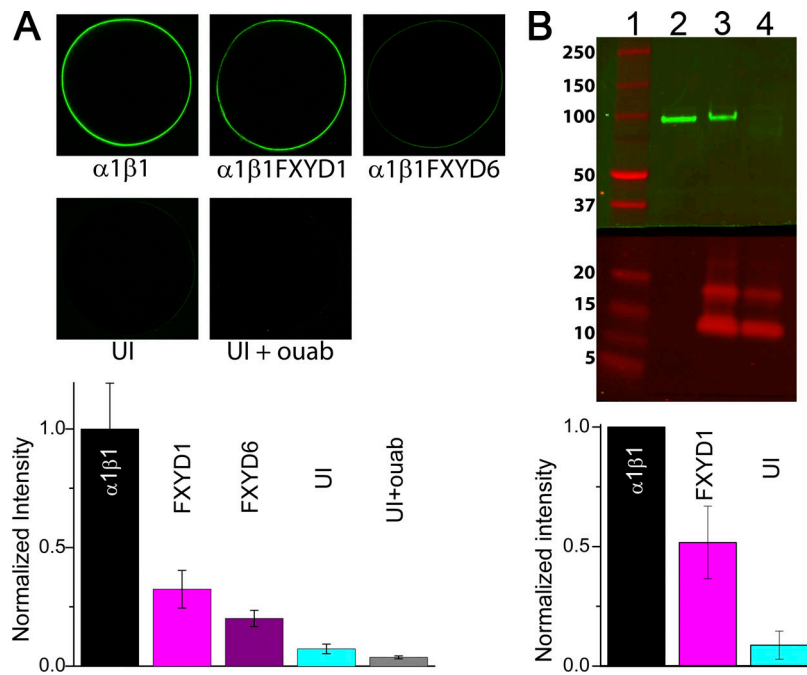


Figure 6. **FXYD1 and FXYD6 reduce pump current.** (A and B) Mean normalized K<sup>+</sup><sub>o</sub>-induced currents from oocytes expressing α1β1 (n = 40) or α1β1FXYD1 (n = 45; A) and for α1β1 (n = 38) or α1β1FXYD6 (n = 29; B). Each group was normalized to the mean outward current from α1β1 oocytes measured the same day or on subsequent days in seven batches of oocytes in each condition. Error bars are SEM. Normalized data points from individual oocytes are shown as open circles. Asterisks indicate significantly different with respect to α1β1 alone by t test, \*\*, P < 0.001.





**Figure 7. Reduced plasma membrane expression of Na/K pumps with FXYD1 and FXYD6.** (A) Confocal image of representative oocytes following incubation in BODIPY FL-ouabain ( $1 \mu\text{M}$ ). Note that preincubation of uninjected oocytes with unlabeled ouabain (UI+ouab) eliminates the signal observed in uninjected oocytes (UI). Fluorescence intensity was measured in two concentric circles (one including the plasma membrane signal) to subtract background fluorescence. The bar graph at the bottom summarizes results from two batches of oocytes (one batch for FXYD6) normalized to the fluorescence intensity measured in oocytes injected with  $\alpha 1\beta 1$  alone. (B) Representative Western blot of plasma membrane preparations from oocytes expressing  $\alpha 1\beta 1$  (lane 2),  $\alpha 1\beta 1\text{FXYD1}$  (lane 3), and FXYD1 alone (lane 4), 3 d after injection (14 oocytes in each condition). The top half was probed with the pan- $\alpha$ -antibody (a5, Developmental Studies Hybridoma Bank) and an anti-mouse secondary antibody (IRDye 800 CW goat anti-mouse; LI-COR). The bottom half was incubated with a polyclonal FXYD1 antibody (ab76597; Abcam) and an anti-rabbit secondary antibody (IRDye 680RD goat anti-rabbit; LI-COR). The bar graphs at the bottom summarize results from five membrane preparations from four oocyte batches, normalized to the intensity of  $\alpha 1\beta 1$  alone. Pump current activated by  $4.5 \text{ mM K}^+$ ,  $145 \text{ mM Na}^+$  in 28  $\alpha 1\beta 1$  and 34  $\alpha 1\beta 1\text{FXYD1}$  oocytes included in these membrane preparations were  $219 \pm 19 \text{ nA}$  and  $100 \pm 10 \text{ nA}$  (mean  $\pm$  SEM), respectively.

patches from oocytes expressing each of the FXYD subunits (Fig. 9 B). The mean  $K_{0.5}$  obtained from Hill plots to individual experiments is shown as a box plot (Fig. 9 C) and listed in Table 3, illustrating that the small effects on the  $K_{0.5}$  for  $\text{Na}^+$  induced by expression of FXYD proteins were not statistically significant from  $\alpha 1\beta 1$  alone.

Results were clearly different when the intracellular solution was designed to approximate the situation in a cell, where  $\text{Na}^+$

would replace the more abundant  $\text{K}^+$  (Fig. 10 and Table 3). Fig. 10 A illustrates representative recordings at zero voltage from patches excised from oocytes expressing  $\alpha 1\beta 1$ , either alone or with each of the FXYD proteins. After measuring the baseline current at each  $\text{Na}^+$  concentration,  $4 \text{ mM MgATP}$  was applied, stimulating an outward current reversibly. As apparent in most traces, the kinetics of pump-current activation at near-saturating  $50 \text{ mM Na}^+$  was also biphasic, but the proportion

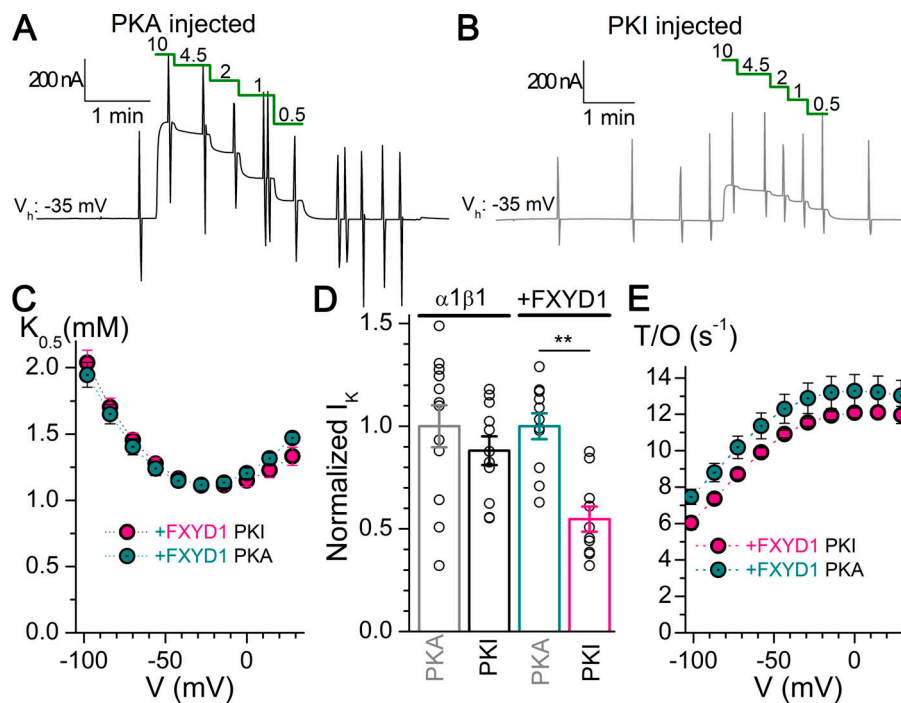


**Figure 8. Effect of PKA on  $\alpha 1\beta 1\text{FXYD1}$  expression and kinetics.** (A and B) Representative recordings of dose-response for  $\text{K}^+$  on oocytes expressing  $\alpha 1\beta 1\text{FXYD1}$  after injection with PKA (A) or PKI (B). (C) Mean  $K_{0.5}$ -V from oocytes expressing  $\alpha 1\beta 1\text{FXYD1}$  injected with PKA ( $n = 20$ ) or PKI ( $n = 19$ ). (D) Mean normalized current induced by  $10 \text{ mM K}^+$  in two batches of oocytes expressing  $\alpha 1\beta 1$  or  $\alpha 1\beta 1\text{FXYD1}$  after injection with PKA or PKI, measured on the same day. Error bars are SEM. Asterisks indicate significantly different at  $P < 0.001$ . (E) Turnover rate in  $4.5 \text{ mM K}^+$  for oocytes expressing  $\alpha 1\beta 1\text{FXYD1}$  injected with PKA ( $n = 10$ ) or PKI ( $n = 10$ ). Error bars are SEM.

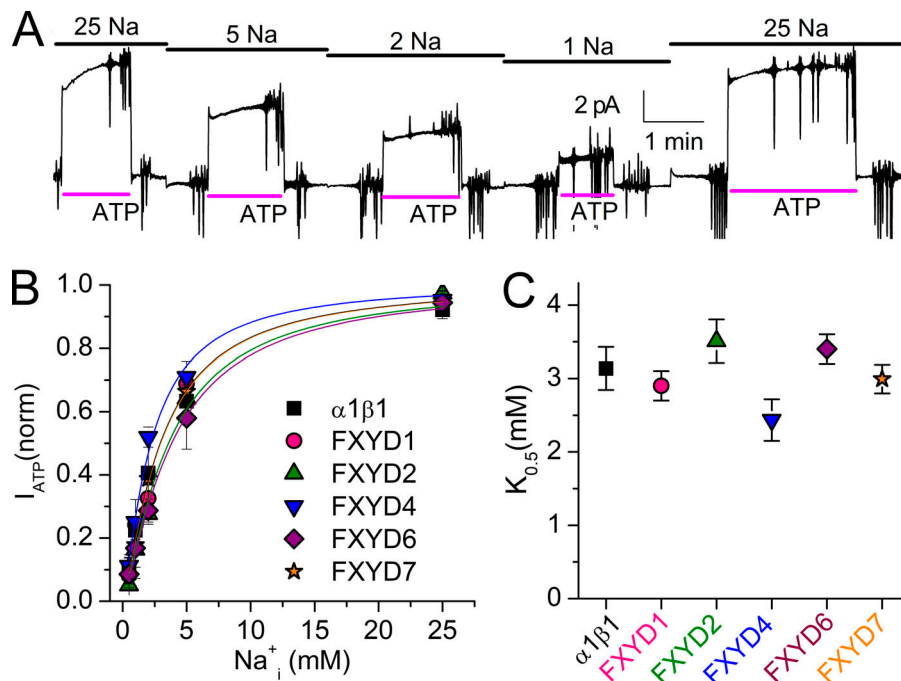


**Figure 9. FXYD effects on Na/K pump interaction with  $\text{Na}^+$  in the presence of NMDG $^+$  (without  $\text{K}^+$ ).** (A) Representative patch from an oocyte expressing  $\alpha 1\beta 1$  alone held at 0 mV with extracellular solution containing 5 mM  $\text{K}^+_{\text{o}}$  in NMDG $^+_{\text{o}}$ . The bars on top indicate  $[\text{Na}^+]_{\text{i}}$  (in mM), and the bars under the traces indicate application of MgATP (4 mM) to activate outward Na/K pump current. Note the biphasic activation, more obvious in first ATP application. Vertical deflections correspond to application of 25-ms-long voltage pulses. (B) Mean ATP-induced current as a function of  $[\text{Na}^+]_{\text{i}}$ . Line plots are Hill equations with the parameters in Table 3. (C)  $K_{0.5, \text{Na}^+}$  for each FXYD. Error bars are SEM.

of slow phase at a given  $\text{Na}^+$  concentration remained more or less constant in subsequent applications of MgATP. A full description of how intracellular ligands influence this slow phase, which has a complex dependence on the time spent with or without nucleotide as well as on the concentrations of both  $\text{Na}^+$  and  $\text{K}^+$  before the addition of MgATP, is currently underway and goes beyond the focus of this article. However, here we mention a few observations that appear to be altered by FXYD proteins. At 50 mM  $\text{Na}^+_{\text{i}}$  with 90 mM  $\text{K}^+_{\text{i}}$ , the slow-phase fraction was  $0.30 \pm 0.13$  ( $n = 26$ ) for  $\alpha 1\beta 1$ ,  $0.43 \pm 0.13$  ( $n = 32$ ) for  $\alpha 1\beta 1\text{FXYD1}$ ,  $0.39 \pm 0.08$  ( $n = 6$ ) for FXYD2,  $0.24 \pm 0.10$  ( $n = 12$ ) for FXYD4,  $0.23 \pm 0.09$  ( $n = 6$ ) for FXYD6, and  $0.11 \pm 0.06$  ( $n = 9$ ) for FXYD7. Application of MgATP at a lower  $\text{Na}^+_{\text{i}}$  concentration (with a concomitant increase in  $\text{K}^+_{\text{i}}$  in this case) generally led to a larger slow-phase fraction (noticeable in the  $\alpha 1\beta 1\text{FXYD1}$  trace and particularly evident in the FXYD2 trace, and less obvious but still visible in traces with other FXYD proteins). At 10 mM  $\text{Na}^+_{\text{i}}$  with 130 mM  $\text{K}^+_{\text{i}}$ , it was  $0.40 \pm 0.11$  ( $n = 20$ ) for  $\alpha 1\beta 1$ ,  $0.50 \pm 0.2$  ( $n = 16$ ) for FXYD1,  $0.70 \pm 0.17$  ( $n = 5$ ) for FXYD2,  $0.37 \pm 0.19$  ( $n = 11$ ) for FXYD4,  $0.46 \pm 0.11$  ( $n = 3$ ) for FXYD6, and  $0.26 \pm 0.12$  ( $n = 8$ ) for FXYD7. Although some small differences did not reach statistical significance for all the FXYD proteins, FXYD1 and FXYD2 appeared to increase the proportion of slow component while FXYD4 and FXYD7 reduced it. For FXYD6, it is difficult to get patches with enough expression due to the trafficking and viability issues induced by this isoform (described above).

Whether the changes in ATP-activation kinetics relate to the changes in overall affinity measured from Hill fits to the  $\text{Na}^+_{\text{i}}$ -concentration dependence of steady-state ATP-activated current (as shown for the mean normalized data in Fig. 10 B) will require a full description of the ion dependence of the slow phase. The apparent affinity for  $\text{Na}^+_{\text{i}}$  was reduced ( $K_{0.5, \text{Na}^+}$  increased) by FXYD1, FXYD2, and FXYD6, while it was increased by FXYD4 and FXYD7 (Fig. 10 C and Table 3); interestingly, these

alterations are in the same direction as the changes in apparent affinity for external  $\text{Na}^+$ . Given that the normal physiological cytoplasmic solution contains high  $[\text{K}^+]_{\text{i}}$ , which raises the  $K_{0.5}$  for  $\text{Na}^+_{\text{i}}$  to values close to the normal  $\text{Na}^+_{\text{i}}$  concentrations (although values vary depending on the cell type and activity level), these results demonstrate that FXYD effects on  $\text{Na}^+_{\text{i}}$  interaction must be analyzed in the presence of  $\text{K}^+_{\text{i}}$  to draw physiologically relevant conclusions. Notably, under these conditions, the observed changes in apparent affinity may have profound consequences for  $\text{Na}^+$  extrusion.

There was a large variability of the  $K_{0.5}$  for  $\alpha 1\beta 1\text{FXYD1}$ -injected oocytes. Both Shapiro-Wilk and Anderson-Darling tests reject the hypothesis that the  $K_{0.5, \text{Na}^+}$  is normally distributed at the 95% confidence level. As FXYD1 is phosphorylated PKA and PKC (Palmer et al., 1991), it is possible that the  $K_{0.5}$  variability reflects two populations of pumps: some that are phosphorylated, showing a relatively high affinity for  $\text{Na}^+_{\text{i}}$ , and some that are dephosphorylated, showing a lower affinity for  $\text{Na}^+_{\text{i}}$ . Na/K pump regulation by PKA-dependent phosphorylation has remained a point of controversy for years (Lu et al., 2016). Several publications using whole-cell preparations reported that activation of the PKA pathway in oocytes (Bibert et al., 2008), ventricular myocytes (Despa et al., 2005; Fuller et al., 2009), and HeLa cells heterologously expressing FXYD1 (Han et al., 2010) increases  $\text{Na}^+_{\text{i}}$  apparent affinity, but similar effects have never been reported in excised patches or isolated membrane preparations (only the effect of FXYD1 phosphomimetic mutations have been reported in purified preparations of Na/K pumps; Mishra et al., 2015).

To determine if PKA affects the apparent  $\text{Na}^+_{\text{i}}$  affinity of  $\alpha 1\beta 1\text{FXYD1}$ , we tried two different approaches. First, we added PKA at 25 mM  $\text{Na}^+_{\text{i}}$ , a subsaturating concentration. In contrast to the expected result arising from an increased apparent affinity for  $\text{Na}^+_{\text{i}}$ , PKA application failed to augment current at 25 mM  $\text{Na}^+_{\text{i}}$  (Fig. 11). However, when 50 mM  $\text{Na}^+_{\text{i}}$  was added after

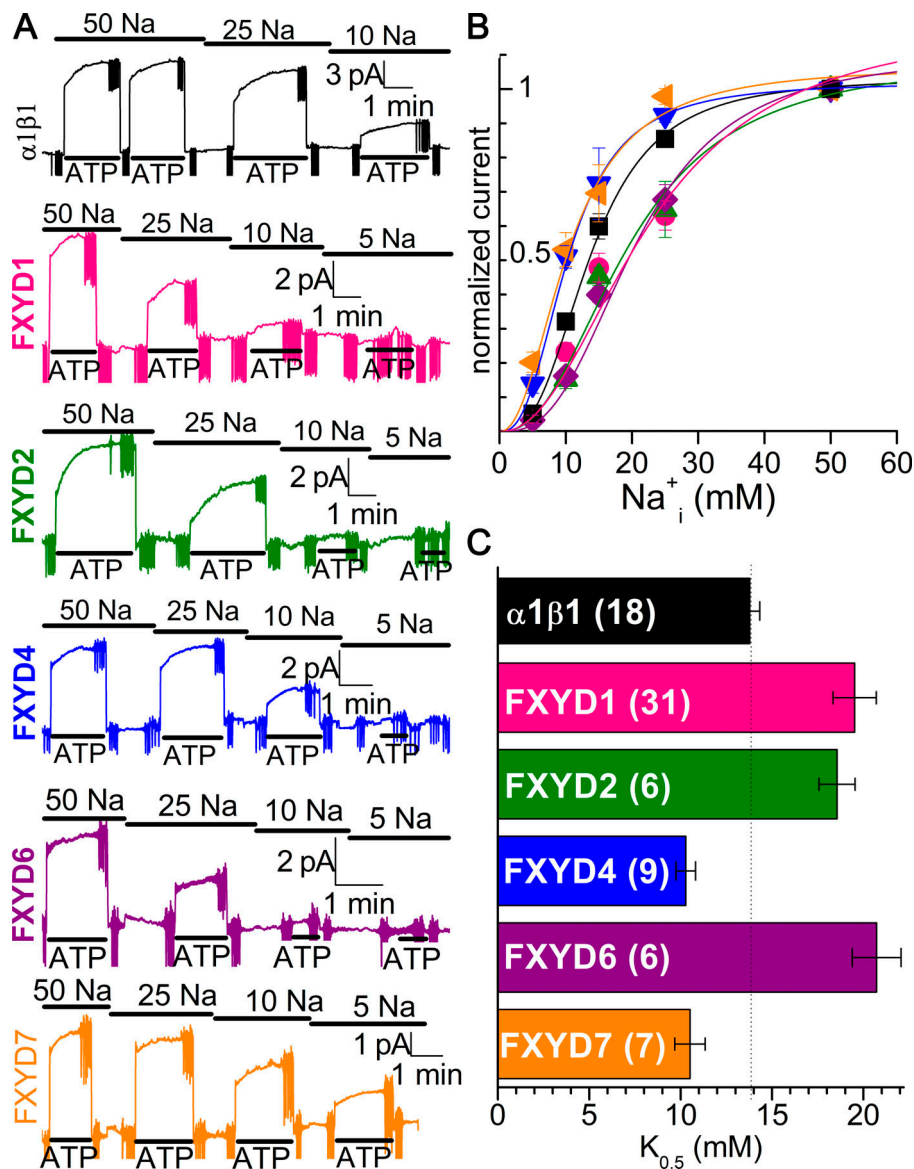


**Figure 10. FXYP effects on Na/K pump interaction with  $Na^+$  in the presence of  $K^+$ .** (A) Patches from oocytes expressing each FXYP protein were held at 0 mV with extracellular solution containing 5 mM  $K^+$  in NMDG. The bars on top indicate  $[Na^+]_i$  (in mM), and the bars under the traces indicate application of MgATP (4 mM) to activate outward Na/K pump current. Vertical deflections correspond to application of 25-ms-long voltage pulses. Note biphasic activation by ATP. (B) Mean ATP-induced current as a function of  $[Na^+]_i$ , normalized to the value at 50 mM  $Na^+$ . Line plots are Hill equations with the parameters in Table 3. (C)  $K_{0.5,Na^+}$  for each FXYP, from the number of experiments in parentheses. Error bars are SEM.

application of PKA, the current increase was smaller than observed in the absence of PKA (Fig. 11 B).

Interpretation of these results is complicated by several aspects. Among them are the possibility that a small rundown of

Na/K pump current in the patch is responsible for the reduction of maximal pump current in the presence of PKA, the unknown rate of FXYP1 phosphorylation by PKA (would 2–3 min in PKA + ATP suffice to phosphorylate all the pumps?), and the also

Table 3. Parameters from Hill fits to  $[Na^+]_i$  dependence, when  $Na^+$  is exchanged with NMDG $^+$  or  $K^+$

Condition	$Na^+$ with NMDG $^+$				$Na^+$ with $K^+$			
	$K_{0.5}$ (mM)	$I_{max}$ (pA)	$H$	$n$	$K_{0.5}$ (mM)	$I_{max}$ (pA)	$H$	$n$
$\alpha 1\beta 1$	$3.1 \pm 0.9$	$7.0 \pm 2.9$	1.2	10	$13.8 \pm 2.3$	$10.2 \pm 3.9$	2.8	18
FXYP1	$2.9 \pm 0.6$	$5.7 \pm 1.6$	1.4	9	$19.5 \pm 6.6^{***}$	$5.6 \pm 1.5$	2.2	31
FXYP2	$3.5 \pm 0.8$	$10.3 \pm 10.3$	1.7	7	$18.1 \pm 2.4^{**}$	$5.3 \pm 0.4$	3.0	6
FXYP4	$2.4 \pm 0.6$	$5.1 \pm 1.2$	1.2	4	$10.4 \pm 1.7^{**}$	$8.5 \pm 5.2$	2.6	9
FXYP6	$3.4 \pm 0.6$	$6.2 \pm 2.5$	1.5	10	$20.7 \pm 3.2^{**}$	$4.6 \pm 0.8$	2.8	6
FXYP7	$3.0 \pm 0.5$	$5.5 \pm 1.0$	1.3	6	$10.5 \pm 2.6^*$	$6.1 \pm 3.0$	2.2	7

Errors represent SD,  $H$  = Hill coefficient, and  $n$  = number of experiments. Significantly different with respect to  $\alpha 1\beta 1$  alone: \*,  $P < 0.01$  and \*\*,  $P < 0.001$  (t test); \*\*\*,  $P < 0.05$  (Mann–Whitney  $U$  test).

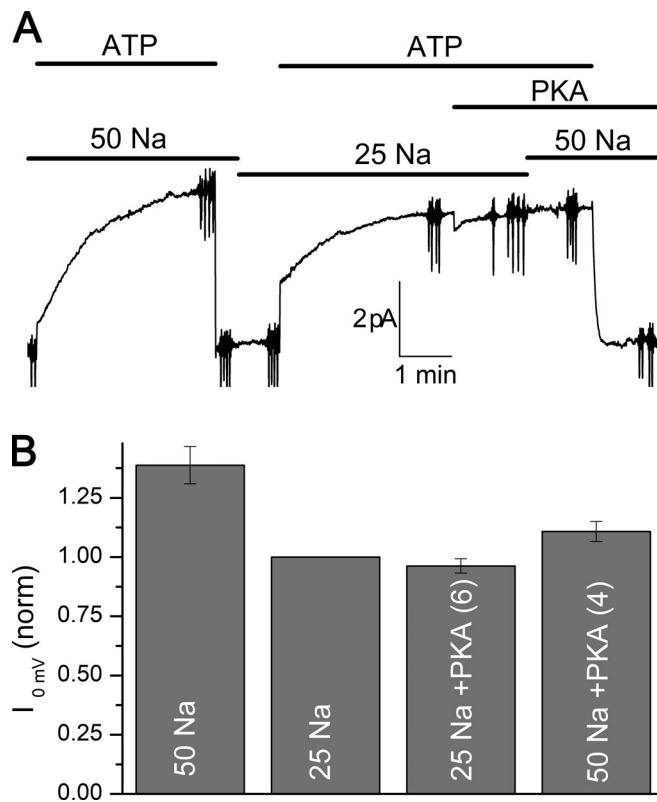


**Figure 11. PKA failed to increase Na/K pump current at 25 mM Na<sup>+</sup><sub>i</sub>.** (A) Na/K pump current was activated by application of ATP in 50 mM and then 25 mM Na<sup>+</sup><sub>i</sub>. After the current reached steady state, PKA was applied at 25 mM Na<sup>+</sup><sub>i</sub> without effect during 2 min. Subsequent application of 50 mM Na<sup>+</sup><sub>i</sub> minimally increased the current. (B) Bar graph summarizing results from six patches (four at 50 mM Na<sup>+</sup><sub>i</sub>) in which similar maneuvers were performed.

unknown FXYP1 dephosphorylation rate by membrane-embedded phosphatases once PKA and/or ATP is withdrawn from the patch. These issues are illustrated in a representative control experiment in which we tested whether the same PKA applied on  $\alpha 1\beta 1$ FXYP1 was capable of activating PKA phosphorylation-dependent CFTR channels, days after performing the pump experiments (Fig. S1). Thus, PKA was indeed active, as it activated CFTR channels in the presence of ATP. In this case, (1) CFTR activation by PKA phosphorylation at multiple sites was slow (i.e., several minutes); (2) channels remained active when they were partially dephosphorylated in the absence of PKA but presence of ATP; and (3) channels were completely deactivated (dephosphorylated) when both ATP and PKA were removed from the patch for 2 min. These phosphorylation and dephosphorylation rates are much harder to estimate in pump-expressing patches. Also, because the experiment was performed in ionic conditions identical to the pump experiments (5 mM K<sup>+</sup><sub>o</sub>, 135 mM NMDG<sup>+</sup><sub>o</sub>, 25 mM Na<sup>+</sup><sub>i</sub>, and 115 mM K<sup>+</sup><sub>i</sub>), but in a patch excised from an oocyte that had previously been incubated in 10  $\mu$ M ouabain, it demonstrates that the outward current activated by ATP in Figs. 9 and 10 is Na/K pump specific.

To limit the incidence of those unknowns, we performed dose-response tests for Na<sup>+</sup><sub>i</sub> in experiments where ATP and PKA were simultaneously present to maximize the times to achieve

PKA-dependent phosphorylation and diminish the uncertainties regarding dephosphorylation. The parameters from Hill fits to those experiments were  $K_{0.5,Na^+} = 15.8 \pm 3.8$ ,  $I_{max} = 6.2 \pm 1.4$  ( $H = 2.4$ ,  $n = 12$ ); the mean  $K_{0.5,Na^+}$  was normally distributed and significantly different from the  $K_{0.5,Na^+}$  with FXYP1 without PKA (Mann-Whitney  $U$  test  $P < 0.05$ ), and not significantly different from patches with  $\alpha 1\beta 1$  alone in a  $t$  test ( $P = 0.24$ ).

## Discussion

Our results provide the first full comparison of the effects of five human FXYP proteins on human  $\alpha 1\beta 1$  in which the experiments were performed in the physiological voltage range with near-physiological conditions under precise control of intracellular and extracellular ion concentrations. The data confirm some, but not all, observations previously reported using isoforms from different species. The most important novel results we describe are (1) that all FXYP isoforms alter the  $E1(3Na^+) \leftrightarrow E2P + 3Na^+$  equilibrium; (2) that all FXYP isoforms alter affinity for Na<sup>+</sup><sub>i</sub>, only in the presence of K<sup>+</sup><sub>i</sub>; (3) that FXYP6 increases the Na/K pump turnover rate; (4) that FXYP1 and FXYP6 reduce the number of Na/K pumps in the plasma membrane; and (5) that PKA application rescues the reduced number of FXYP1-Na/K pumps in the plasma membrane and appears to reverse FXYP1 effects on Na<sup>+</sup><sub>i</sub> affinity.

### FXYP effects on extracellular ion affinities

All FXYP subunit isoforms have been shown previously to alter Na/K pump function (Geering, 2008), something we also observed with the five human FXYP isoforms we studied. They all alter the apparent affinity for transported ions, but in many cases, the relatively mild effects on interaction with K<sup>+</sup><sub>o</sub> reported were altered by the presence of Na<sup>+</sup><sub>o</sub>. In some cases, distinct results from experiments using interspecies isoform interactions were reported (Béguin et al., 1997). FXYP effects on partial reactions that only bind Na<sup>+</sup><sub>o</sub> had not been reported previously.

Many of the pioneering studies by the Geering laboratory (Geering, 2006) determined the effect of FXYP isoforms from one species on Na/K pumps from a different species in batrachian ionic conditions. Nonetheless, our observations on  $K_{0.5}$  for K<sup>+</sup><sub>o</sub> in the presence of Na<sup>+</sup><sub>o</sub> are similar to Geering's observations: FXYP1 produces a small, voltage-independent increase in  $K_{0.5,K^+}$  (Crambert et al., 2002) and FXYP2 and FXYP6 have nominal effects, whereas FXYP4 (Béguin et al., 2001) and FXYP7 (Béguin et al., 2002) induce a voltage-dependent increase of  $K_{0.5,K^+}$  at negative voltages (probably indicative of their ability to increase the apparent affinity for competing Na<sup>+</sup><sub>o</sub>). Frequently, the direction of the effects on the apparent affinity for K<sup>+</sup><sub>o</sub> varies depending on whether Na<sup>+</sup><sub>o</sub> is present. FXYP1 is the only auxiliary subunit that seems to have similar effects in the presence or absence of Na<sup>+</sup><sub>o</sub> (Béguin et al., 2001, 2002; Crambert et al., 2002, 2005; Delprat et al., 2007; Lindzen et al., 2003b; Pu et al., 2001; Stanley et al., 2015).

Our results measuring Na<sup>+</sup>-dependent transient charge movement (partial reactions inside the dashed box in Fig. 1 B) help clarify the complications caused by ion (i.e., substrate) competition. The center of the voltage-dependent distribution of



this charge movement reflects the pump's overall apparent affinity for  $\text{Na}^+$ . We observed statistically significant shifts of the Q-V curves by each FXYP protein (Fig. 4 B and Table 2): to the right with FXYP4 (+30 mV) and FXYP7 (+20 mV) and to the left by FXYP2 (−30 mV), FXYP6 (−20 mV), and FXYP1 (−10 mV), which indicates an approximately twofold increase or decrease in apparent affinity for  $\text{Na}^+$ , per 25-mV shift to the right or to the left, respectively (Moreno et al., 2020). A previous report measuring the effect of cow FXYP2 on sheep  $\alpha 1\beta 1$  did not observe a shift of the Q-V curve (Dempski et al., 2008). It is possible that the FXYP2 effect was lost either due to the use of isoform subunits from different species, the left-shifted nature of this  $\alpha 1\beta 1$  construct's Q-V curve compared with others (compare Stanley et al., 2018), or significant differences in 6 of 18 intracellular domain residues between cow and human FXYP2.

The findings regarding apparent affinity for  $\text{Na}^+$  are all consistent with previous reports indicating that the effects on  $K_{0.5} \text{K}^+$  were largely shaped by the presence or absence of  $\text{Na}^+$ . For example, FXYP1 was reported to slightly reduce the apparent affinity for  $\text{K}^+$  in the absence of  $\text{Na}^+$ , but surprisingly, its effects on  $\alpha 1\beta 1$  in the presence of  $\text{Na}^+$  were voltage independent (Crambert et al., 2002). The mild effect of FXYP1 on the voltage-dependent apparent affinity for  $\text{Na}^+$  that we observe explains why it does not alter the voltage dependence of the  $K_{0.5, \text{K}^+}$  in the presence of  $\text{Na}^+$ , as the voltage-dependent apparent affinity for  $\text{Na}^+$  is reduced to the same degree as the apparent affinity for  $\text{K}^+$ .

The affinity for  $\text{Na}^+$  or  $\text{K}^+$  is the product of the coordination efficiency of the ion-binding sites as well as the fraction of enzyme residing in E1 (with increased  $\text{Na}^+$  affinity) versus E2 (with increased  $\text{K}^+$  affinity). Apparent ion affinities are further complicated by the inherent competition between  $\text{Na}^+$  and  $\text{K}^+$  in the two major conformations. Even within a single major conformation (i.e., E1 or E2), apparent affinities as well as selectivity can be altered if, for example, the preference between individual E2 states is modified. More specifically, effects on apparent affinities and ion selectivity would be quite different depending on whether FXYP proteins favor occupancy of the empty E2P, the fully occluded E2( $2\text{K}^+$ ), or the partially occluded E2P( $2\text{Na}^+$ ).

The transient charge movement kinetics provides mechanistic insight into which partial reactions may be modified by FXYPs. All FXYP subunits altered the proportion of total charge moved in the slow component (Fig. 3 and Table 2). FXYP1, FXYP2, and FXYP6 reduced the fraction of the total charge moving in the slow component, while FXYP4 and FXYP7 increased it. Because these slow charge movements are thought to represent the binding of the last  $\text{Na}^+$  in the backward direction (i.e., reocclusion) or release of the first  $\text{Na}^+$  in the forward direction (deocclusion; Gadsby et al., 2012; Hilgemann, 1994; Holmgren et al., 2000), this may be interpreted as suggesting that the equilibrium constant for interaction of the last  $\text{Na}^+$  to bind is altered by all FXYP subunits, albeit in different directions and to different degrees. However, this effect can be mediated simply by altering the  $\text{E1} \leftrightarrow \text{E2}$  equilibrium instead of the actual ion-binding reaction.

Presently, we can state that at negative voltages (−100 mV), FXYP2 and FXYP1 reduced the rate of rebinding/reocclusion

(i.e., the “backward” transition  $\text{E2P} + 3 \text{Na}^+ \rightarrow \text{E1P}(3\text{Na}^+)$ ; Fig. 1 B) by ~50% and ~20%, respectively. These effects appear to be sufficient to account for their respective ~50% and ~30% reduction in overall apparent  $\text{Na}^+$  affinity. On the other hand, FXYP6 reduces the apparent affinity for  $\text{Na}^+$  by ~50%, both by accelerating ~25% the  $\text{Na}^+$  deocclusion/release step (i.e., the “forward” transition from  $\text{E1P}(3\text{Na}^+) \rightarrow \text{E2P} + 3 \text{Na}^+$ ; Fig. 1 B) as well as by reducing ~20% the reocclusion rate. FXYP4 increased the  $\text{Na}^+$  rebinding/occlusion rate ~30% and perhaps led to a small ~10% reduction in the deocclusion rate (not statistically significant given the small difference), while FXYP7 reduced the deocclusion rate ~25%. In any case, determinations of reocclusion rates at very negative voltages may be limited by the inherent slow clamp of the TEVC technique.

The small changes observed in apparent affinity for  $\text{K}^+$  (~20–40%; Table 1) are consistent with previous reports and unlikely to be physiologically relevant in the regulation of  $\alpha 1\beta 1$  pumps under normal serum concentrations, where Na/K pumps will mostly be functioning at  $\text{K}^+$  concentrations that are four to five times larger than the  $K_{0.5}$ . However, the conditions would change if pumps were located in special compartments. For instance, the  $\text{K}^+$  concentration of the cerebrospinal fluid bathing pumps interacting with FXYP6, FXYP7, and FXYP1 in central nervous system neurons varies between 2.5 and 10 mM depending on neuronal activity, with basal values of 2.5–3 mM  $\text{K}^+$  (Bradbury and Davson, 1965; Cserr, 1965; Keep et al., 1993). If  $\alpha 1\beta 1$  pumps normally associate with FXYP7 in neurons (Béguin et al., 2002), these would be functioning near the  $K_{0.5, \text{K}^+}$  at neuronal resting potentials and drastically activated when there is a need to clear  $\text{K}^+$  after its concentration is increased by neuronal activity.

A similar substantial physiological importance would arise if FXYP proteins interact with pumps formed by the  $\alpha 2$  subunit, as FXYP1 is known to do (Bossuyt et al., 2005), because  $\alpha 2$  pumps have a much lower apparent affinity for external  $\text{K}^+$  in the presence of external  $\text{Na}^+$  (DiFranco et al., 2015; Stanley et al., 2015; Stoica et al., 2017), particularly when associated with  $\beta 2$  (Hilbers et al., 2016; Stanley et al., 2015), its preferred  $\beta$ -isoform association partner (Tokhtaeva et al., 2012). Indeed, FXYP1 reduces the  $K_{0.5}$  for  $\text{K}^+$  in  $\alpha 2\beta 2$  pumps from ~5.5 to ~8 mM at 0 mV (compare Fig. 8 in Stanley et al., 2015), something that would transform  $\alpha 2\beta 2$  pumps into a reservoir for  $\text{K}^+$ , clearing at depolarized potentials. Clearing  $\text{K}^+$  by  $\alpha 2$  pumps is essential in skeletal muscle T-tubules and glia following periods of high electrical activity. Therefore, whether the pumps are associated with FXYP1 could have a dramatic effect on their effectiveness as a pumping reservoir. Nevertheless, it remains unclear whether distinct FXYP isoforms have a predilection for different  $\alpha$ -subunit isoforms in the cells in which they are expressed.

FXYP2 and FXYP4 are well known to associate with  $\alpha 1\beta 1$  in the basolateral membrane of the thick ascending limb (Arystarkhova et al., 2002) and the principal cells of the medullary collecting duct (Capurro et al., 1996), respectively. Therefore, their small effects on  $\text{K}^+$  apparent affinity are probably innocuous, and their main importance comes from their effect on  $\text{Na}^+$  affinity, as the Na/K pumps in the collecting duct

will drive the reabsorption of  $\text{Na}^+$  at lower intracellular concentrations.

### FXYP effects on intracellular ion affinities

In contrast to effects on  $K_{0.5,K^+}$ , the small effects of FXYPs on the apparent affinity for  $\text{Na}^+_i$  would have profound physiological impact because Na/K pumps function at  $\text{Na}^+_i$  concentrations near the  $K_{0.5,\text{Na}^+}$  value, and because the high cooperativity of pump current activation by  $\text{Na}^+_i$  results in very steep  $\text{Na}^+_i$  dependencies. Under normal physiological intracellular ion concentrations, all five FXYP proteins significantly altered the apparent affinity for  $\text{Na}^+_i$  (Fig. 10 and Table 3). These alterations can be divided into two groups: (1) those that increase  $\text{Na}^+_i$  apparent affinity, reducing the  $K_{0.5}$  by  $\sim 30\%$  (FXYP4 and FXYP7); and (2) those that reduce apparent affinity, increasing the  $K_{0.5}$  by  $\sim 30\%$  (FXYP1, FXYP2, and FXYP6). To illustrate the importance of the changes in apparent affinity for  $\text{Na}^+_i$  we describe here, in physiological terms, if the  $\text{Na}^+_i$  concentration in the cell remained constant at 14 mM, the high cooperativity of  $\text{Na}^+_i$  activation ( $nH \sim 2.8$  mM) means that the “small” increase in  $K_{0.5,\text{Na}^+}$  from 14 to 20 mM due to association of  $\alpha 1\beta 1$  pumps with FXYP1, FXYP2, or FXYP6 would manifest as a nearly threefold reduction in effective pumping capacity. On the other hand, a decrease in  $K_{0.5,\text{Na}^+}$  from 14 to 10 mM due to association of  $\alpha 1\beta 1$  pumps with FXYP4 or FXYP7 would mean a 35% increase in pumping capacity.

The  $K_{0.5}$  values for  $\text{Na}^+_i$  in the presence of  $\text{K}^+_i$  reported here agree with reports from the Geering laboratory for FXYP1 (Crambert et al., 2002), FXYP2 (Béguin et al., 1997; Pu et al., 2001), FXYP4 (Béguin et al., 2001; Lindzen et al., 2003b), and FXYP6 (Delprat et al., 2007) but contrast with the lack of change in  $\text{Na}^+_i$  apparent affinity reported for FXYP7 by Béguin et al. (2002). This difference may be because Béguin et al. (2002) reported the effect of mouse FXYP7 on rat  $\alpha 1\beta 1$  instead of human FXYP7 on human  $\alpha 1\beta 1$  or because of the uncertainty of the  $\text{Na}^+_i$  and  $\text{K}^+_i$  concentrations in their study (as intracellular concentrations cannot be directly controlled in a whole oocyte) versus the precise control of intracellular solutions in our patch experiments.

An important observation for all FXYPs is that the changes in apparent affinity for  $\text{Na}^+_i$  disappear in the absence of  $\text{K}^+$ . Therefore, our studies at near-mammalian cationic concentrations (140 mM  $\text{Na}^+_i + \text{K}^+_i$ ) indicate that this relevant physiological effect of FXYP proteins effectively requires altering the competition between  $\text{K}^+_i$  and  $\text{Na}^+_i$ . In keeping with our observation, Pu et al. (2001) previously reported that FXYP2 decreased the apparent affinity for  $\text{Na}^+_i$  by increasing antagonism (competition) from  $\text{K}^+_i$ . Taken together, these results indicate that FXYP proteins may act by altering ion selectivity of the Na/K pump at intracellular-facing sites rather than by changing the actual affinity for one ion.

It is important to note that the effects on  $\text{Na}^+_i$  apparent affinity in the presence of  $\text{K}^+$  are in the same direction as the effects on extracellular  $\text{Na}^+$  apparent affinity in the absence of competitor. Although it is tempting to conclude that this is due to an increased affinity for the third  $\text{Na}^+$  site (site III, the site that interacts only with  $\text{Na}^+$ ), the need for  $\text{K}^+_i$  antagonism to observe

the effect of FXYP isoforms on  $\text{Na}^+_i$  apparent affinity does not require direct effects on ion-binding sites. A nonmutually exclusive alternative explanation can be surmised from the effect of each particular FXYP on transient charge movement (Figs. 4 and 5 and Table 2). FXYP4, and to a lesser extent FXYP7, favor the occupancy of the third  $\text{Na}^+$  from the extracellular side and a shift to the E1P(3 $\text{Na}^+$ ) conformation, while FXYP2 and FXYP6, and to a lesser extent FXYP1, reduce binding of that third extracellular  $\text{Na}^+$  and favor the E2P conformation. An effect on the E1P/E2P equilibrium suffices to explain the changes in apparent affinity for extracellular  $\text{Na}^+$ , because their effects on ion binding and conformational equilibrium are inseparable with the experiments presented here. Future studies will attempt to dissect direct effects on ion binding from effects on the major conformational equilibrium using techniques with faster time resolution or that report conformational changes concomitantly with the electric signals, such as voltage clamp fluorometry (Stanley et al., 2018).

A modification of the E1/E2 equilibrium by FXYP proteins can also explain the required antagonism by  $\text{K}^+$  to observe their effect on the apparent affinity for  $\text{Na}^+_i$ . If we assume that the ion-free enzyme is poised toward E1 whether FXYP isoforms are present or not, any preference for the backward transition from E1(empty) to E2(2K) would be realized only when  $\text{K}^+_i$  is added, concomitantly amplifying the action of FXYP on  $K_{0.5,\text{Na}^+}$ . Therefore, only in the presence of  $\text{K}^+_i$  to move the pump back to E2(K2), will FXYP isoforms that promote occupancy of E2 reduce apparent affinity for  $\text{Na}^+_i$ , whereas FXYP proteins that stabilize E1 will increase the apparent affinity for  $\text{Na}^+_i$ . Although this model completely explains all our observations and is strongly supported by the transient charge movement data, it must be noted that it contrasts with a previous proposal that FXYP2 increases E1 occupancy (Pu et al., 2001).

Another argument in favor of altering the E1/E2 conformational equilibrium comes from the Na/K pump crystal structures. There, FXYP proteins are seen interacting with transmembrane segment 9, too far from the ion-binding sites formed by residues in transmembrane segments 4, 5, 6, and 8 to directly alter ion binding (Kanai et al., 2013; Morth et al., 2007). This indicates that their effects on ion binding are allosteric, something that could be achieved simply by modification of the conformational state of the protein.

The ATP-activation kinetics measured in patches may also lend additional support to FXYP proteins acting by altering the equilibrium between E1 and E2. Activation of pump current by ATP in the presence of  $\text{K}^+_i$  is clearly biphasic, with a fast phase (limited by our tens-of-milliseconds solution exchange system) followed by a slow phase with a time constant in the tens of seconds. Each FXYP protein appears to alter the fraction of current in the slow component (Fig. 10 A). FXYP1 and FXYP2, which slow entrance to E1P(3 $\text{Na}^+$ ) in transient currents and reduce apparent affinity for  $\text{Na}^+_i$ , increase the fraction of the slow component. Conversely, FXYP4 and FXYP7, which favor E1P(3 $\text{Na}^+$ ) in the transient currents and raise the apparent affinity for  $\text{Na}^+_i$ , reduced the fraction of slow phase (The data for FXYP6 have been more difficult to obtain due to lower expression). One plausible explanation for the observed biphasic ATP

activation time course is that when ATP is absent (i.e., before pump cycle activation) the enzyme system rests in equilibrium between the E2(2K<sup>+</sup>)-occluded and the E1-3 Na<sup>+</sup>-bound states (compare Fig. 1 B). Then, as ATP is added, pumps in E1 with 3 Na<sup>+</sup> bound can cycle immediately, while pumps in the E2(2K<sup>+</sup>) state must first deocclude K<sup>+</sup> before they can start cycling. If this was the case, the slow time constant observed would appear to be well below the transport rates of ~15–30 s<sup>-1</sup> in our conditions at room temperature (Fig. 8 E; Crambert et al., 2000; Meyer et al., 2017) and ~100 s<sup>-1</sup> in ventricular myocytes at 36°C (Friedrich et al., 1996).

Interestingly, previous descriptions from patches from ventricular myocytes in the absence of K<sub>i</sub> show fast activation by ATP in all but the first ATP application (Friedrich et al., 1996). Although less drastic, a similar behavior was observed in our patches (Fig. 9). As both our experiments and those of Friedrich et al. (1996) began with excision of the patch into K<sup>+</sup>-containing solutions without ATP, it is plausible that the first activation by ATP reflects the pumps leaving an E2(2K<sup>+</sup>) state with the slow component we describe here, but further experiments will be required to directly address this possibility.

The importance of studies to describe in detail the slow transitions that depend on the presence of transported ions is highlighted by the recent observation of a Na<sub>i</sub> depletion-triggered inactivated state described by Hilgemann (2020b). The appearance of the slow activation phase in patches, just like the entrance into the inactivated state in whole-cell experiments, is dramatically influenced by the presence of competing K<sub>i</sub> (Lu and Hilgemann, 2017). Therefore, it is possible that the slow ATP-activation phase we describe here represents the inactive state entered by Na/K pumps when the Na<sub>i</sub> concentration is reduced in whole-cell patch-clamp experiments with ventricular myocytes (Hilgemann, 2020b; Lu and Hilgemann, 2017). If this is the case, the changes in apparent ion selectivity of intracellular-facing pumps induced by FXYP proteins that we describe here would have profound consequences on Na/K pump activity. Notably, the preference of intracellular-facing sites for K<sub>i</sub> over Na<sub>i</sub> is increased in the presence of FXYP1, FXYP2, and FXYP6, while the fraction of pumps in the inactive form is increased in myocytes expressing FXYP1 compared with FXYP1 knockouts (Hilgemann, 2020b; Lu et al., 2016). An important difference between experiments in cells and our experiments is that ATP is present to drive the pump to E1, thus competing with K<sup>+</sup> driving the pump back to E2 in the whole-cell experiment, while the slow phase we describe here is induced by the combined presence of K<sub>i</sub> and absence of ATP. Yet, in the absence of Na<sub>i</sub> and the presence of ATP, K<sub>i</sub> still drives a substantial portion of pumps to E2 (Gatto et al., 2005). Thus, it is tempting to speculate both that the slow phase represents the inactivated state described by Hilgemann (2020b) and that the effects of FXYP proteins on intracellular ion affinities reflect their modulation of these inactive states. In the future, it will be important to directly evaluate whether this slow activating phase in excised patches corresponds to the Na<sub>i</sub> depleted-inactivated state, whether the entrance to the inactivated state is favored by long occupancies of E2 conformations, and/or whether the effects of FXYP proteins, which regulate Na/K

pump ion selectivity and modify ATP-activation kinetics, reflect alteration of the inactivated state's occupancy.

### Does PKA phosphorylation modulate FXYP1's effect on ion affinities?

Na/K pump regulation by phosphorylation remains controversial (Hilgemann, 2020b; Lu et al., 2016). Reports in whole cells have shown that activation of the PKA pathway in oocytes (Bibert et al., 2008), ventricular myocytes (Despa et al., 2005; Fuller et al., 2009), and HeLa cells heterologously expressing FXYP1 (Han et al., 2010) augment Na/K pump current due to an increase in apparent affinity for Na<sub>i</sub>. In contrast, Fine et al. (2013) show that PKA pathway stimulation had no effect on pump currents in iCell Cardiomyocytes at 9 mM Na<sub>i</sub>, although the experiments were performed without K<sub>i</sub>, a condition with higher apparent affinity, where the reduction in apparent affinity by FXYP1 should not be observed (Table 3).

Direct application of PKA failed to increase the pump current at one subsaturating Na<sub>i</sub>; increased pump current would be expected if phosphorylation increases the apparent affinity for Na<sub>i</sub> concentration. The inability to observe this increase in isolated membrane preparations has led other groups to propose that a yet-unknown intracellular factor is required for this effect (Hilgemann, 2020a). However, it is also possible that the absence of a direct increase in current by PKA in the patches arises from the complications related to unknown phosphorylation/dephosphorylation rates in the isolated membrane system, which complicate experimental design. In our hands, when experiments measuring dose effect for Na<sub>i</sub> were performed with simultaneous application of PKA and ATP, the apparent affinity of α1β1FXYP1 pumps for Na<sub>i</sub> appeared to be increased in a statistically significant manner. Further experiments will be required to resolve this conundrum, for instance, by analyzing direct effects of PKA at lower Na<sub>i</sub> concentrations, in the presence of phosphatase inhibitors, and on patches expressing Ser/Thr-phosphorylation-site mutants.

### FXYP6 increases α1β1 turnover rate

In the presence of physiological 4.5 mM K<sub>o</sub>, FXYP6 increases the turnover rate in a voltage-dependent manner (by 50% at -80 mV and 25% at +40 mV). Because FXYP6 significantly accelerates the rate of transient charge movement at positive potentials (Figs. 3 and 4 A), a transition independent from the extracellular Na<sub>o</sub> concentration (Holmgren and Rakowski, 2006; Holmgren et al., 2000; Nakao and Gadsby, 1986), the observed increased turnover rate probably reflects FXYP6's true increase to the rate of Na<sub>o</sub> deocclusion during the E1P(3Na) ↔ E2P + 3 Na<sub>o</sub> transition, which is one of the two rate-limiting steps in the pump cycle. The stronger effect at negative voltages reflects the reduced affinity for Na<sub>o</sub> of FXYP6-associated Na/K pumps (i.e., a left-shifted Q-V; Fig. 4 B). That is, FXYP6 simultaneously speeds up Na<sub>o</sub> deocclusion and reduces sensitivity to the Na<sub>o</sub> rebinding that competes with K<sub>o</sub> for the externally accessible binding sites.

No other FXYP protein tested here had such a drastic effect on the rate of Na<sub>o</sub> deocclusion or the turnover rate of pump cycling, although FXYP1 appeared to reduce the turnover rate at



0 mV to a much lower extent. A previous study reported that FXYD5 may be another FXYD protein that increases the turnover rate (Lubarski et al., 2005), but this was based on measurements of ionic currents of mouse FXYD5 with rat  $\alpha 1$  and pig  $\beta 1$ , and without normalizing Na/K pump activity to the number of pumps in the plasma membrane. Confirmation will require measurements like those we present here in human  $\alpha 1\beta 1$ FXYD5.

It is interesting to note that FXYD6 is an inhibitor of  $\alpha 1\beta 1$  in terms of  $\text{Na}^+$  binding, but an activator in terms of turnover rate. Consequently, these qualities may allow FXYD6-associated pumps to respond when  $\text{Na}^+$  is increased, such as during neurotransmission in the brain where FXYD6 is primarily expressed (Kadowaki et al., 2004). The increased turnover rate would also allow for larger pumping capacity, which may be especially useful for regulating larger  $\text{Na}^+$  increases. However, as described above for FXYD1, this observation applies only to the association of FXYD6 with  $\alpha 1$  pumps. Additional effects of FXYD6 on ion transport may well depend on whether it associates with and regulates the  $\alpha 3$  isoform in neurons. Association of FXYD6 and  $\alpha 3$  in oocytes has been demonstrated (Delprat et al., 2007), but whether it alters the transport properties of  $\alpha 3$  pumps has yet to be reported. Future studies will address these important questions.

The most striking observation regarding regulation of  $\alpha 1\beta 1$  by FXYD6 in our oocyte system is its astonishing  $\sim 70\%$  reduction of plasma membrane expression of  $\alpha 1\beta 1$  (Figs. 6 and 7). No such observations were conveyed in previous reports determining the effects of mouse FXYD6 coexpressed with rat isoforms in *Xenopus* oocytes (Delprat et al., 2007). It is possible that this discrepancy reflects that mouse and human FXYD6 differ at two intracellular residues near two cysteines, which have been deemed essential for FXYD1 regulation by palmitoylation (Tulloch et al., 2011). However, a prevalent intracellular location of FXYD6 location was reported in nondifferentiated PC12 cells (compare Fig. 3 in Delprat et al., 2007).

#### Regulation of $\alpha 1\beta 1$ expression by FXYD1 and PKA

Like FXYD6, FXYD1 reduced  $\alpha 1\beta 1$ -pump density at the oocyte plasma membrane by  $\sim 50\%$  (Fig. 6 and Fig. 7). The original description of FXYD1's effects by Geering's group shows a small reduction of  $I_{\text{max}}$  on the third day of expression, probably just below statistical significance (compare Fig. 4 in Crambert et al., 2002). In a subsequent study, the same group showed identical maximal Na/K pump currents from rat or human isoforms, regardless of whether the oocytes expressed FXYD1 (Bibert et al., 2008). The differences may reflect the injection of different total cRNA for all three isoforms, differences in the isoforms, or differences in the oocyte culture solutions used. Reports of studies comparing Na/K pump currents between ventricular myocytes from wild-type and FXYD1-knockout mice are also conflicting; some show an increase in Na/K pump current density in FXYD1 knockout (Pavlović et al., 2007) mice, while others show a decrease (Han et al., 2009).

Upon injection of the catalytic subunit of PKA into oocytes expressing FXYD1, we observed a 30–50% increase in  $\alpha 1\beta 1$ FXYD1 Na/K pump surface expression, indicated by larger Na/K pump currents, without turnover rate variation (Fig. 8). Bibert et al.

(2008) reported that when the PKA-activation pathway was stimulated, the maximal current did not change in oocytes expressing human or rat  $\alpha 1\beta 1$  and dog FXYD1. Our differing results may be explained by (1) the fact that Bibert et al. (2008) did not observe the reduced expression in the presence of unphosphorylated FXYD1 (which may be required to observe the increase in expression by activation of PKA), (2) the different approach we used here (i.e., directly injecting PKA instead of activating the PKA pathway with forskolin or epinephrine), and/or (3) the use of different species of the  $\alpha \beta$  and FXYD isoforms.

Conflicting results regarding stimulation of the PKA pathway have been described in myocytes; Silverman et al., (2005) showed an increase in Na/K pump current in guinea pig ventricular myocytes voltage clamped with the perforated patch technique, while others reported unchanged Na/K pump current amplitude (Despa et al., 2005; Fine et al., 2013). It is plausible that PKA-induced delivery of new Na/K pumps to the plasma membrane requires a cellular component that is lost in regular whole-cell patch-clamp experiments, but not with perforated patches (containing all cytosolic constituents) or whole oocytes under voltage clamp.

FXYD1 is known to be retained in the endoplasmic reticulum in some expression systems (Lansbery et al., 2006), and coexpression of PKA increases its delivery to the plasma membrane (Mounsey et al., 1999). More recently, FXYD1 was reported to regulate trafficking of aquaporins (Arystarkhova et al., 2017). Inconsistencies in the literature regarding Na/K pump regulation by FXYD1 may relate to cell-specific issues, including the existence of phosphorylation-dependent FXYD1 pools that are not associated with Na/K pumps (Wypijewski et al., 2013), but more probably highlight the fact that regulation of Na/K pump is very complex (Lu et al., 2016) and may involve endocytosis events that are linked to oxidative stress and ischemia-reperfusion injury (Fine et al., 2011; Hilgemann and Fine, 2011; Lariccia et al., 2011; Lin et al., 2013), which may vary depending on the contents of whole-cell patch pipettes or the cell isolation and cell culture procedures used. In any case, the ability of PKA to increase both the apparent  $\text{Na}^+$  affinity and the plasma membrane insertion of  $\alpha 1\beta 1$ FXYD1 pumps would have dramatic implications for  $\text{Na}^+$  regulation in response to sympathetic stimulation, as these effects would drastically increase both the affinity of  $\text{Na}^+$  and the  $\text{Na}^+$ -extrusion capacity.

#### FXYD proteins alter membrane stability and traffic

Our results showing retention of  $\alpha 1\beta 1$  Na/K pumps by association with FXYD1 and FXYD6 point to these two proteins as regulators of Na/K pump trafficking. In this respect, Tulloch et al. (2011) reported that inhibition of the Na/K pump by FXYD1 requires palmitoylation and that palmitoylation increases FXYD1's half-life in the membrane. It is possible that palmitoylation of FXYD1 contributes to its recently reported membrane stabilization of  $\alpha 2$  Na/K pumps (Lifshitz et al., 2007). Furthermore, palmitoylation drives massive endocytosis events in response to oxidation insults during ischemia reperfusion in the heart (Hilgemann et al., 2013; Lin et al., 2013). Heavy palmitoylation of FXYD1, controlled by the mitochondria, suggests it may be a driver for these drastic trafficking changes. The



structural features that allow protein recognition by palmitoyltransferases are mostly unknown (Greaves and Chamberlain, 2011) and are only beginning to be elucidated (Howie et al., 2014).

Considering that FXYD1's palmitoylatable cysteines (C60 and C62) and nearly all of the immediate surrounding amino acids are conserved in FXYD6 (Fig. 1 A), it might be expected that FXYD6 is also functionally regulated via palmitoylation. In addition, Fig. 1 A shows that both cysteines are conserved in FXYD4, while the second cysteine is conserved in FXYD2 and FXYD7 (the first cysteine is conserved in FXYD5 and both are conserved in FXYD3, the isoforms not evaluated here). However, the residues surrounding the cysteines in these FXYDs are less conserved relative to FXYD1. Additionally, glutathionylation of FXYD cysteines was shown to regulate Na/K pump activity (Bibert et al., 2011), which adds even more complexity to the nature of Na/K pump regulation. The intricate regulatory role of FXYD cysteines, together with other aspects of the structure-function relationships that determine the functional differences among FXYDs described here, which likely include interactions with anionic phospholipids (Cornelius and Mahmoud, 2007) and possibly with other membrane proteins (Zhang et al., 2009), will be the subject of future studies.

## Acknowledgments

Joseph A. Mindell served as editor.

This work was supported by grants from the National Science Foundation (MCB-1515434) and the National Institute of Neurological Disorders and Stroke (1-R03 NS116433-01) to P. Artigas and a predoctoral fellowship from the American Heart Association (17PRE32860001) to D.J. Meyer. C. Gatto was supported by National Institutes of Health grant GM061583.

The authors declare no competing financial interests.

Author contributions: D.J. Meyer designed research, performed and analyzed experiments and wrote the paper, M. De Sautu, S. Bijlani, K. Spontarelli and V.C. Young performed and analyzed experiments, C. Gatto, designed research and wrote the paper, P. Artigas designed research, preformed and analyzed experiments and wrote the paper.

Submitted: 15 May 2020

Accepted: 29 October 2020

## References

Artigas, P., S.J. Al'aref, E.A. Hobart, L.F. Díaz, M. Sakaguchi, S. Straw, and O.S. Andersen. 2006. 2,3-butanedione monoxime affects cystic fibrosis transmembrane conductance regulator channel function through phosphorylation-dependent and phosphorylation-independent mechanisms: the role of bilayer material properties. *Mol. Pharmacol.* 70: 2015–2026. <https://doi.org/10.1124/mol.106.026070>

Arystarkhova, E., R.K. Wetzel, and K.J. Sweadner. 2002. Distribution and oligomeric association of splice forms of Na<sup>+</sup>-K<sup>+</sup>-ATPase regulatory gamma-subunit in rat kidney. *Am. J. Physiol. Renal Physiol.* 282: F393–F407. <https://doi.org/10.1152/ajprenal.00146.2001>

Arystarkhova, E., R. Bouley, Y.B. Liu, and K.J. Sweadner. 2017. Impaired AQP2 trafficking in Fxyd1 knockout mice: A role for FXYD1 in regulated vesicular transport. *PLoS One*. 12:e0188006.

Attali, B., H. Latter, N. Rachamim, and H. Garty. 1995. A corticosteroid-induced gene expressing an "IsK-like" K<sup>+</sup> channel activity in Xenopus

oocytes. *Proc. Natl. Acad. Sci. USA*. 92:6092–6096. <https://doi.org/10.1073/pnas.92.13.6092>

Béguin, P., G. Crambert, S. Guennoun, H. Garty, J.D. Horisberger, and K. Geering. 2001. CHIF, a member of the FXYD protein family, is a regulator of Na,K-ATPase distinct from the gamma-subunit. *EMBO J.* 20: 3993–4002. <https://doi.org/10.1093/emboj/20.15.3993>

Béguin, P., G. Crambert, F. Monnet-Tschudi, M. Uldry, J.D. Horisberger, H. Garty, and K. Geering. 2002. FXYD7 is a brain-specific regulator of Na,K-ATPase alpha 1-beta isozymes. *EMBO J.* 21:3264–3273. <https://doi.org/10.1093/emboj/cdf330>

Béguin, P., X. Wang, D. Firsov, A. Puoti, D. Claeys, J.D. Horisberger, and K. Geering. 1997. The gamma subunit is a specific component of the Na,K-ATPase and modulates its transport function. *EMBO J.* 16:4250–4260. <https://doi.org/10.1093/emboj/16.14.4250>

Bibert, S., C.C. Liu, G.A. Figtree, A. Garcia, E.J. Hamilton, F.M. Marassi, K.J. Sweadner, F. Cornelius, K. Geering, and H.H. Rasmussen. 2011. FXYD proteins reverse inhibition of the Na<sup>+</sup>-K<sup>+</sup> pump mediated by glutathionylation of its beta1 subunit. *J. Biol. Chem.* 286:18562–18572. <https://doi.org/10.1074/jbc.M110.184101>

Bibert, S., S. Roy, D. Schaer, J.D. Horisberger, and K. Geering. 2008. Phosphorylation of phospholemman (FXYD1) by protein kinases A and C modulates distinct Na,K-ATPase isozymes. *J. Biol. Chem.* 283:476–486. <https://doi.org/10.1074/jbc.M705830200>

Blanco, G. 2005. Na,K-ATPase subunit heterogeneity as a mechanism for tissue-specific ion regulation. *Semin. Nephrol.* 25:292–303. <https://doi.org/10.1016/j.semnephrol.2005.03.004>

Blanco, G., J.C. Koster, G. Sánchez, and R.W. Mercer. 1995. Kinetic properties of the alpha 2 beta 1 and alpha 2 beta 2 isozymes of the Na,K-ATPase. *Biochemistry*. 34:319–325. <https://doi.org/10.1021/bi00001a039>

Bossuyt, J., X. Ai, J.R. Moorman, S.M. Pogwizd, and D.M. Bers. 2005. Expression and phosphorylation of the na-pump regulatory subunit phospholemman in heart failure. *Circ. Res.* 97:558–565. <https://doi.org/10.1161/01.RES.0000181172.27931.c3>

Bossuyt, J., S. Despa, F. Han, Z. Hou, S.L. Robia, J.B. Lingrel, and D.M. Bers. 2009. Isoform specificity of the Na/K-ATPase association and regulation by phospholemman. *J. Biol. Chem.* 284:26749–26757. <https://doi.org/10.1074/jbc.M109.047357>

Bradbury, M.W., and H. Davson. 1965. The transport of potassium between blood, cerebrospinal fluid and brain. *J. Physiol.* 181:151–174. <https://doi.org/10.1113/jphysiol.1965.sp007752>

Capurro, C., N. Coutry, J.P. Bonvalet, B. Escoubet, H. Garty, and N. Farman. 1996. Cellular localization and regulation of CHIF in kidney and colon. *Am. J. Physiol.* 271:C753–C762. <https://doi.org/10.1152/ajprenal.1996.271.3.C753>

Castillo, J.P., D. De Giorgis, D. Basilio, D.C. Gadsby, J.J. Rosenthal, R. Latorre, M. Holmgren, and F. Bezanilla. 2011. Energy landscape of the reactions governing the Na<sup>+</sup> deeply occluded state of the Na<sup>+</sup>/K<sup>+</sup>-ATPase in the giant axon of the Humboldt squid. *Proc. Natl. Acad. Sci. USA*. 108: 20556–20561. <https://doi.org/10.1073/pnas.1116439108>

Cornelius, F., and Y.A. Mahmoud. 2007. Modulation of FXYD interaction with Na,K-ATPase by anionic phospholipids and protein kinase phosphorylation. *Biochemistry*. 46:2371–2379. <https://doi.org/10.1021/bi062239j>

Crambert, G., M. Fuzesi, H. Garty, S. Karlsh, and K. Geering. 2002. Phospholemman (FXYD1) associates with Na,K-ATPase and regulates its transport properties. *Proc. Natl. Acad. Sci. USA*. 99:11476–11481. <https://doi.org/10.1073/pnas.182267299>

Crambert, G., U. Hasler, A.T. Beggah, C. Yu, N.N. Modyanov, J.D. Horisberger, L. Lelièvre, and K. Geering. 2000. Transport and pharmacological properties of nine different human Na, K-ATPase isozymes. *J. Biol. Chem.* 275:1976–1986. <https://doi.org/10.1074/jbc.275.3.1976>

Crambert, G., C. Li, D. Claeys, and K. Geering. 2005. FXYD3 (Mat-8), a new regulator of Na,K-ATPase. *Mol. Biol. Cell.* 16:2363–2371. <https://doi.org/10.1091/mbc.e04-10-0878>

Cserr, H. 1965. Potassium exchange between cerebrospinal fluid, plasma, and brain. *Am. J. Physiol.* 209:1219–1226. <https://doi.org/10.1152/ajplegacy.1965.209.6.1219>

Dascal, N. 2000. Voltage Clamp Recordings from Xenopus Oocytes. *Curr. Protoc. Neurosci.* 10:Chapter 6:Unit 6.12.

Delprat, B., D. Schaer, S. Roy, J. Wang, J.L. Puel, and K. Geering. 2007. FXYD6 is a novel regulator of Na,K-ATPase expressed in the inner ear. *J. Biol. Chem.* 282:7450–7456. <https://doi.org/10.1074/jbc.M609872200>

Dempski, R.E., J. Lustig, T. Friedrich, and E. Bamberg. 2008. Structural arrangement and conformational dynamics of the gamma subunit of the Na<sup>+</sup>/K<sup>+</sup>-ATPase. *Biochemistry*. 47:257–266. <https://doi.org/10.1021/bi701799b>

- Despa, S., J. Bossuyt, F. Han, K.S. Ginsburg, L.G. Jia, H. Kutchai, A.L. Tucker, and D.M. Bers. 2005. Phospholemman-phosphorylation mediates the beta-adrenergic effects on Na/K pump function in cardiac myocytes. *Circ. Res.* 97:252–259. <https://doi.org/10.1161/01.RES.0000176532.97731.e5>
- DiFranco, M., H. Hakimjavadi, J.B. Lingrel, and J.A. Heiny. 2015. Na,K-ATPase  $\alpha 2$  activity in mammalian skeletal muscle T-tubules is acutely stimulated by extracellular  $K^+$ . *J. Gen. Physiol.* 146:281–294. <https://doi.org/10.1085/jgp.201511407>
- Feschchenko, M.S., C. Donnet, R.K. Wetzel, N.K. Asinowski, L.R. Jones, and K.J. Sweadner. 2003. Phospholemman, a single-span membrane protein, is an accessory protein of Na,K-ATPase in cerebellum and choroid plexus. *J. Neurosci.* 23:2161–2169.
- Fine, M., M.C. Llaguno, V. Lariccia, M.J. Lin, A. Yaradanakul, and D.W. Hilgemann. 2011. Massive endocytosis driven by lipidic forces originating in the outer plasmalemmal monolayer: a new approach to membrane recycling and lipid domains. *J. Gen. Physiol.* 137:137–154. <https://doi.org/10.1085/jgp.201010469>
- Fine, M., F.-M. Lu, M.-J. Lin, O. Moe, H.-R. Wang, and D.W. Hilgemann. 2013. Human-induced pluripotent stem cell-derived cardiomyocytes for studies of cardiac ion transporters. *Am. J. Physiol. Cell Physiol.* 305: C481–C491. <https://doi.org/10.1152/ajpcell.00143.2013>
- Forbush, B. III, J.H. Kaplan, and J.F. Hoffman. 1978. Characterization of a new photoaffinity derivative of ouabain: labeling of the large polypeptide and of a proteolipid component of the Na, K-ATPase. *Biochemistry.* 17: 3667–3676. <https://doi.org/10.1021/bi00610a037>
- Friedrich, T., E. Bamberg, and G. Nagel. 1996.  $Na^+, K^+$ -ATPase pump currents in giant excised patches activated by an ATP concentration jump. *Bioophys. J.* 71:2486–2500. [https://doi.org/10.1016/S0006-3495\(96\)79442-0](https://doi.org/10.1016/S0006-3495(96)79442-0)
- Fuller, W., J. Howie, L.M. McLatchie, R.J. Weber, C.J. Hastie, K. Burness, D. Pavlovic, and M.J. Shattock. 2009. FXYP1 phosphorylation in vitro and in adult rat cardiac myocytes: threonine 69 is a novel substrate for protein kinase C. *Am. J. Physiol. Cell Physiol.* 296:C1346–C1355. <https://doi.org/10.1152/ajpcell.00523.2008>
- Gadsby, D.C., F. Bezanilla, R.F. Rakowski, P. De Weer, and M. Holmgren. 2012. The dynamic relationships between the three events that release individual  $Na^+$  ions from the  $Na^+/K^+$ -ATPase. *Nat. Commun.* 3:669. <https://doi.org/10.1038/ncomms1673>
- Gatto, C., J.B. Helms, M.C. Prasse, K.L. Arnett, and M.A. Milanick. 2005. Kinetic characterization of tetrapropylammonium inhibition reveals how ATP and Pi alter access to the  $Na^+-K^+$ -ATPase transport site. *Am. J. Physiol. Cell Physiol.* 289:C302–C311. <https://doi.org/10.1152/ajpcell.00043.2005>
- Geering, K. 2006. FXYP proteins: new regulators of Na,K-ATPase. *Am. J. Physiol. Renal Physiol.* 290:F241–F250. <https://doi.org/10.1152/ajprenal.00126.2005>
- Geering, K. 2008. Functional roles of Na,K-ATPase subunits. *Curr. Opin. Nephrol. Hypertens.* 17:526–532. <https://doi.org/10.1097/MNH.0b013e3283036cbf>
- Greaves, J., and L.H. Chamberlain. 2011. DHHC palmitoyl transferases: substrate interactions and (patho)physiology. *Trends Biochem. Sci.* 36: 245–253. <https://doi.org/10.1016/j.tibs.2011.01.003>
- Han, F., J. Bossuyt, J.L. Martin, S. Despa, and D.M. Bers. 2010. Role of phospholemman phosphorylation sites in mediating kinase-dependent regulation of the  $Na^+-K^+$ -ATPase. *Am. J. Physiol. Cell Physiol.* 299: C1363–C1369. <https://doi.org/10.1152/ajpcell.00027.2010>
- Han, F., A.L. Tucker, J.B. Lingrel, S. Despa, and D.M. Bers. 2009. Extracellular potassium dependence of the  $Na^+-K^+$ -ATPase in cardiac myocytes: isoform specificity and effect of phospholemman. *Am. J. Physiol. Cell Physiol.* 297:C699–C705. <https://doi.org/10.1152/ajpcell.00063.2009>
- Hilbers, F., W. Kopec, T.J. Isaksen, T.H. Holm, K. Lykke-Hartmann, P. Nissen, H. Khandelia, and H. Poulsen. 2016. Tuning of the Na,K-ATPase by the beta subunit. *Sci. Rep.* 6:20442. <https://doi.org/10.1038/srep20442>
- Hilgemann, D.W. 1994. Channel-like function of the Na,K pump probed at microsecond resolution in giant membrane patches. *Science.* 263: 1429–1432. <https://doi.org/10.1126/science.8128223>
- Hilgemann, D.W. 1997. Cytoplasmic ATP-dependent regulation of ion transporters and channels: mechanisms and messengers. *Annu. Rev. Physiol.* 59:193–220. <https://doi.org/10.1146/annurev.physiol.59.1.193>
- Hilgemann, D.W. 2020a. Control of cardiac contraction by sodium: Promises, reckonings, and new beginnings. *Cell Calcium.* 85:102129. <https://doi.org/10.1016/j.ceca.2019.102129>
- Hilgemann, D.W. 2020b. Regulation of ion transport from within ion transit pathways. *J. Gen. Physiol.* 152:e201912455. <https://doi.org/10.1085/jgp.201912455>
- Hilgemann, D.W., and M. Fine. 2011. Mechanistic analysis of massive endocytosis in relation to functionally defined surface membrane domains. *J. Gen. Physiol.* 137:155–172. <https://doi.org/10.1085/jgp.201010470>
- Hilgemann, D.W., M. Fine, M.E. Linder, B.C. Jennings, and M.J. Lin. 2013. Massive endocytosis triggered by surface membrane palmitoylation under mitochondrial control in BHK fibroblasts. *eLife.* 2:e01293. <https://doi.org/10.7554/eLife.01293>
- Holmgren, M., and R.F. Rakowski. 2006. Charge translocation by the  $Na^+/K^+$  pump under  $Na^+/Na^+$  exchange conditions: intracellular  $Na^+$  dependence. *Biophys. J.* 90:1607–1616. <https://doi.org/10.1529/biophysj.105.072942>
- Holmgren, M., J. Wagg, F. Bezanilla, R.F. Rakowski, P. De Weer, and D.C. Gadsby. 2000. Three distinct and sequential steps in the release of sodium ions by the  $Na^+/K^+$ -ATPase. *Nature.* 403:898–901. <https://doi.org/10.1038/35002599>
- Howie, J., L. Reilly, N.J. Fraser, J.M. Vlachaki Walker, K.J. Wypijewski, M.L. Ashford, S.C. Calaghan, H. McClafferty, L. Tian, M.J. Shipston, et al. 2014. Substrate recognition by the cell surface palmitoyl transferase DHHC5. *Proc. Natl. Acad. Sci. USA.* 111:17534–17539. <https://doi.org/10.1073/pnas.1413627111>
- Ino, Y., M. Gotoh, M. Sakamoto, K. Tsukagoshi, and S. Hirohashi. 2002. Dysadherin, a cancer-associated cell membrane glycoprotein, down-regulates E-cadherin and promotes metastasis. *Proc. Natl. Acad. Sci. USA.* 99:365–370. <https://doi.org/10.1073/pnas.012452999>
- Jaisser, F., P. Jaunin, K. Geering, B.C. Rossier, and J.D. Horisberger. 1994. Modulation of the Na,K-pump function by beta subunit isoforms. *J. Gen. Physiol.* 103:605–623. <https://doi.org/10.1085/jgp.103.4.605>
- Kadowaki, K., K. Sugimoto, F. Yamaguchi, T. Song, Y. Watanabe, K. Singh, and M. Tokuda. 2004. Phosphohippolin expression in the rat central nervous system. *Brain Res. Mol. Brain Res.* 125:105–112. <https://doi.org/10.1016/j.molbrainres.2004.03.021>
- Kanai, R., H. Ogawa, B. Vilsen, F. Cornelius, and C. Toyoshima. 2013. Crystal structure of a  $Na^+$ -bound  $Na^+, K^+$ -ATPase preceding the E1P state. *Nature.* 502:201–206. <https://doi.org/10.1038/nature12578>
- Keep, R.F., J. Xiang, and A. Lorris Betz. 1993. Potassium Transport at the Blood-Brain and Blood-CSF Barriers. In *Frontiers in Cerebral Vascular Biology: Transport and Its Regulation*. L.R. Drewes, and A.L. Betz, editors. Springer US, Boston, MA. 43–54. [https://doi.org/10.1007/978-1-4615-2920-0\\_8](https://doi.org/10.1007/978-1-4615-2920-0_8)
- Lansbery, K.L., L.C. Burcea, M.L. Mendenhall, and R.W. Mercer. 2006. Cytoplasmic targeting signals mediate delivery of phospholemman to the plasma membrane. *Am. J. Physiol. Cell Physiol.* 290:C1275–C1286.
- Lariccia, V., M. Fine, S. Magi, M.J. Lin, A. Yaradanakul, M.C. Llaguno, and D.W. Hilgemann. 2011. Massive calcium-activated endocytosis without involvement of classical endocytic proteins. *J. Gen. Physiol.* 137:111–132. <https://doi.org/10.1085/jgp.201010468>
- Li, C., G. Crambert, D. Thuillard, S. Roy, D. Schaer, and K. Geering. 2005. Role of the transmembrane domain of FXYP7 in structural and functional interactions with Na,K-ATPase. *J. Biol. Chem.* 280:42738–42743. <https://doi.org/10.1074/jbc.M508451200>
- Lifshitz, Y., E. Petrovich, H. Haviv, R. Goldshleger, D.M. Tal, H. Garty, and S.J. Karlish. 2007. Purification of the human  $\alpha 2$  isoform of Na,K-ATPase expressed in *Pichia pastoris*. Stabilization by lipids and FXYP1. *Biochemistry.* 46:14937–14950. <https://doi.org/10.1021/bi701812c>
- Lin, M.J., M. Fine, J.Y. Lu, S.L. Hofmann, G. Frazier, and D.W. Hilgemann. 2013. Massive palmitoylation-dependent endocytosis during reoxygenation of anoxic cardiac muscle. *eLife.* 2:e01295. <https://doi.org/10.7554/eLife.01295>
- Lindzen, M., R. Aizman, Y. Lifshitz, M. Füzesi, S.J. Karlish, and H. Garty. 2003a. Domains involved in the interactions between FXYP and Na,K-ATPase. *Ann. N. Y. Acad. Sci.* 986:530–531. <https://doi.org/10.1111/j.1749-6632.2003.tb07242.x>
- Lindzen, M., R. Aizman, Y. Lifshitz, I. Lubarski, S.J. Karlish, and H. Garty. 2003b. Structure-function relations of interactions between Na,K-ATPase, the gamma subunit, and corticosteroid hormone-induced factor. *J. Biol. Chem.* 278:18738–18743. <https://doi.org/10.1074/jbc.M213253200>
- Lu, F.M., and D.W. Hilgemann. 2017. Na/K pump inactivation, subsarcolemmal Na measurements, and cytoplasmic ion turnover kinetics contradict restricted Na spaces in murine cardiac myocytes. *J. Gen. Physiol.* 149:727–749. <https://doi.org/10.1085/jgp.20171780>
- Lu, F.M., C. Deisl, and D.W. Hilgemann. 2016. Profound regulation of Na/K pump activity by transient elevations of cytoplasmic calcium in murine cardiac myocytes. *eLife.* 5:e19267. <https://doi.org/10.7554/eLife.19267>
- Lubarski, I., K. Pihakaski-Maunsbach, S.J. Karlish, A.B. Maunsbach, and H. Garty. 2005. Interaction with the Na,K-ATPase and tissue distribution

- of FXYD5 (related to ion channel). *J. Biol. Chem.* 280:37717–37724. <https://doi.org/10.1074/jbc.M506397200>
- Mercer, R.W., D. Biemesderfer, D.P. Bliss Jr., J.H. Collins, and B. Forbush III. 1993. Molecular cloning and immunological characterization of the gamma polypeptide, a small protein associated with the Na,K-ATPase. *J. Cell Biol.* 121:579–586. <https://doi.org/10.1083/jcb.121.3.579>
- Meyer, D.J., C. Gatto, and P. Artigas. 2017. On the effect of hyperaldosteronism-inducing mutations in Na/K pumps. *J. Gen. Physiol.* 149:1009–1028. <https://doi.org/10.1085/jgp.201711827>
- Meyer, D.J., C. Gatto, and P. Artigas. 2019. Na/K Pump Mutations Associated with Primary Hyperaldosteronism Cause Loss of Function. *Biochemistry.* 58:1774–1785. <https://doi.org/10.1021/acs.biochem.9b00051>
- Mishra, N.K., M. Habeck, C. Kirchner, H. Haviv, Y. Peleg, M. Eisenstein, H.J. Apell, and S.J. Karlsh. 2015. Molecular Mechanisms and Kinetic Effects of FXYD1 and Phosphomimetic Mutants on Purified Human Na,K-ATPase. *J. Biol. Chem.* 290:28746–28759. <https://doi.org/10.1074/jbc.M115.687913>
- Moorman, J.R., C.J. Palmer, J.E. John III, M.E. Durieux, and L.R. Jones. 1992. Phospholemman expression induces a hyperpolarization-activated chloride current in *Xenopus* oocytes. *J. Biol. Chem.* 267:14551–14554.
- Moreno, C., S. Yano, F. Bezanilla, R. Latorre, and M. Holmgren. 2020. Transient Electrical Currents Mediated by the Na<sup>+</sup>/K<sup>+</sup>-ATPase: A Tour from Basic Biophysics to Human Diseases. *Biophys. J.* 119:236–242. <https://doi.org/10.1016/j.bpj.2020.06.006>
- Morrison, B.W., J.R. Moorman, G.C. Kowdley, Y.M. Kobayashi, L.R. Jones, and P. Leder. 1995. Mat-8, a novel phospholemman-like protein expressed in human breast tumors, induces a chloride conductance in *Xenopus* oocytes. *J. Biol. Chem.* 270:2176–2182. <https://doi.org/10.1074/jbc.270.5.2176>
- Morth, J.P., B.P. Pedersen, M.S. Toustrup-Jensen, T.L. Sørensen, J. Petersen, J.P. Andersen, B. Vilsen, and P. Nissen. 2007. Crystal structure of the sodium-potassium pump. *Nature.* 450:1043–1049. <https://doi.org/10.1038/nature06419>
- Mounsey, J.P., K.P. Lu, M.K. Patel, Z.H. Chen, L.T. Horne, J.E. John III, A.R. Means, L.R. Jones, and J.R. Moorman. 1999. Modulation of *Xenopus* oocyte-expressed phospholemman-induced ion currents by co-expression of protein kinases. *Biochim. Biophys. Acta.* 1451:305–318.
- Nakao, M., and D.C. Gadsby. 1986. Voltage dependence of Na translocation by the Na/K pump. *Nature.* 323:628–630. <https://doi.org/10.1038/323628a0>
- Palmer, C.J., B.T. Scott, and L.R. Jones. 1991. Purification and complete sequence determination of the major plasma membrane substrate for cAMP-dependent protein kinase and protein kinase C in myocardium. *J. Biol. Chem.* 266:11126–11130.
- Pavlović, D., W. Fuller, and M.J. Shattock. 2007. The intracellular region of FXYD1 is sufficient to regulate cardiac Na/K ATPase. *FASEB J.* 21:1539–1546. <https://doi.org/10.1096/fj.06-7269com>
- Price, E.M., and J.B. Lingrel. 1988. Structure-function relationships in the Na,K-ATPase alpha subunit: site-directed mutagenesis of glutamine-111 to arginine and asparagine-122 to aspartic acid generates a ouabain-resistant enzyme. *Biochemistry.* 27:8400–8408. <https://doi.org/10.1021/bi00422a016>
- Pu, H.X., F. Cluzeaud, R. Goldshleger, S.J. Karlsh, N. Farman, and R. Blostein. 2001. Functional role and immunocytochemical localization of the gamma a and gamma b forms of the Na,K-ATPase gamma subunit. *J. Biol. Chem.* 276:20370–20378. <https://doi.org/10.1074/jbc.M010836200>
- Silverman, B., W. Fuller, P. Eaton, J. Deng, J.R. Moorman, J.Y. Cheung, A.F. James, and M.J. Shattock. 2005. Serine 68 phosphorylation of phospholemman: acute isoform-specific activation of cardiac Na/K ATPase. *Cardiovasc. Res.* 65:93–103. <https://doi.org/10.1016/j.cardiores.2004.09.005>
- Stanley, C.M., D.G. Gagnon, A. Bernal, D.J. Meyer, J.J. Rosenthal, and P. Artigas. 2015. Importance of the Voltage Dependence of Cardiac Na/K ATPase Isozymes. *Biophys. J.* 109:1852–1862. <https://doi.org/10.1016/j.bpj.2015.09.015>
- Stanley, K.S., D.J. Meyer, C. Gatto, and P. Artigas. 2016. Intracellular Requirements for Passive Proton Transport through the Na<sup>+</sup>/K<sup>+</sup>-ATPase. *Biophys. J.* 111:2430–2439. <https://doi.org/10.1016/j.bpj.2016.09.042>
- Stanley, K.S., V.C. Young, C. Gatto, and P. Artigas. 2018. External Ion Access in the Na/K Pump: Kinetics of Na<sup>+</sup>, K<sup>+</sup>, and Quaternary Amine Interaction. *Biophys. J.* 115:361–374. <https://doi.org/10.1016/j.bpj.2018.06.007>
- Stoica, A., B.R. Larsen, M. Assentoft, R. Holm, L.M. Holt, F. Vilhardt, B. Vilsen, K. Lykke-Hartmann, M.L. Olsen, and N. MacAulay. 2017. The  $\alpha 2\beta 2$  isoform combination dominates the astrocytic Na<sup>+</sup>/K<sup>+</sup>-ATPase activity and is rendered nonfunctional by the  $\alpha 2$ .G301R familial hemiplegic migraine type 2-associated mutation. *Glia.* 65:1777–1793. <https://doi.org/10.1002/glia.23194>
- Tokhtaeva, E., R.J. Clifford, J.H. Kaplan, G. Sachs, and O. Vagin. 2012. Subunit isoform selectivity in assembly of Na,K-ATPase  $\alpha$ - $\beta$  heterodimers. *J. Biol. Chem.* 287:26115–26125. <https://doi.org/10.1074/jbc.M112.370734>
- Tulloch, L.B., J. Howie, K.J. Wypijewski, C.R. Wilson, W.G. Bernard, M.J. Shattock, and W. Fuller. 2011. The inhibitory effect of phospholemman on the sodium pump requires its palmitoylation. *J. Biol. Chem.* 286:36020–36031. <https://doi.org/10.1074/jbc.M111.282145>
- Vedovato, N., and D.C. Gadsby. 2010. The two C-terminal tyrosines stabilize occluded Na/K pump conformations containing Na or K ions. *J. Gen. Physiol.* 136:63–82. <https://doi.org/10.1085/jgp.201010407>
- Wypijewski, K.J., J. Howie, L. Reilly, L.B. Tulloch, K.L. Aughton, L.M. McLatchie, M.J. Shattock, S.C. Calaghan, and W. Fuller. 2013. A separate pool of cardiac phospholemman that does not regulate or associate with the sodium pump: multimers of phospholemman in ventricular muscle. *J. Biol. Chem.* 288:13808–13820. <https://doi.org/10.1074/jbc.M113.460956>
- Yaragatupalli, S., J.F. Olivera, C. Gatto, and P. Artigas. 2009. Altered Na<sup>+</sup> transport after an intracellular alpha-subunit deletion reveals strict external sequential release of Na<sup>+</sup> from the Na/K pump. *Proc. Natl. Acad. Sci. USA.* 106:15507–15512. <https://doi.org/10.1073/pnas.0903752106>
- Zhang, X.Q., J. Wang, L.L. Carl, J. Song, B.A. Ahlers, and J.Y. Cheung. 2009. Phospholemman regulates cardiac Na<sup>+</sup>/Ca<sup>2+</sup> exchanger by interacting with the exchanger's proximal linker domain. *Am. J. Physiol. Cell Physiol.* 296:C911–C921. <https://doi.org/10.1152/ajpcell.00196.2008>

## Supplemental material



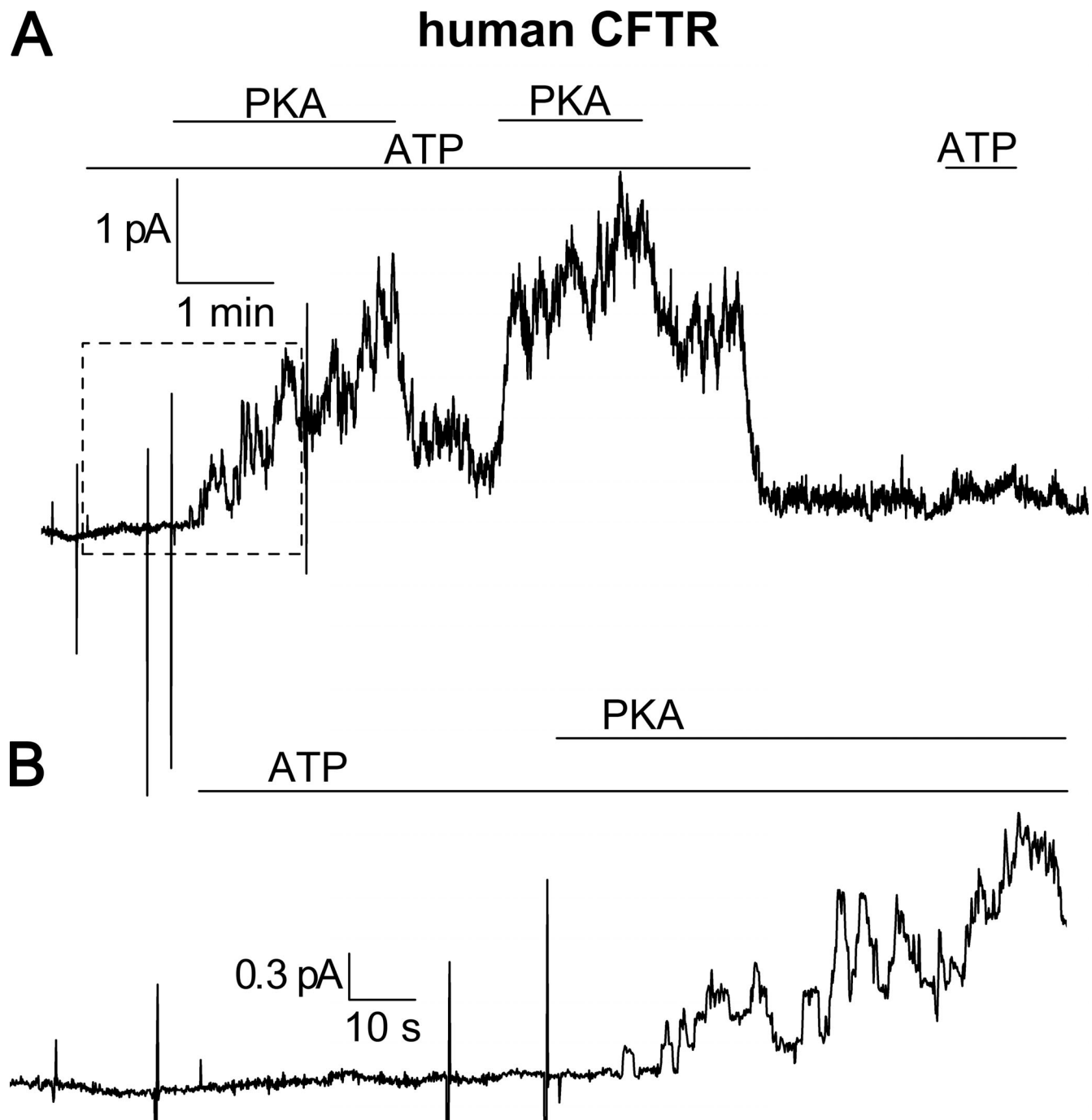


Figure S1. **CFTR recording in a giant patch demonstrating PKA activity.** As a positive control for the patch-clamp experiments on  $\alpha 1\beta 1\text{FX}1\text{YD}1$ , we tested the ability of the same preparation of PKA to activate CFTR, typically a few days after the  $\alpha 1\beta 1\text{FX}1\text{YD}1$  recordings. **(A)** Current recording at 0 mV from a large, inside-out patch excised from an oocyte 1 d after injection with human CFTR cRNA. Endogenous Na/K pumps were inhibited by incubating the oocyte in 10  $\mu\text{M}$  ouabain before the experiment. The pipette contained the same external NMDG<sup>+</sup> solution with 5 mM K<sup>+</sup> as other patch clamp experiments, and the inside of the patch was perfused with 25 mM Na<sup>+</sup> internal solution ( $[\text{Na}^+] + [\text{K}^+] = 140 \text{ mM}$ ). Under these experimental conditions ( $\sim 150 \text{ mM}$  external Cl<sup>-</sup> and  $\sim 30 \text{ mM}$  internal Cl<sup>-</sup>, 0 mV), CFTR currents are outward. Application of 4 mM ATP alone to the inside of the patch produced no change in the baseline current, but simultaneous application of ATP with 10  $\mu\text{M}$  PKA catalytic subunit induced an outward current that returned to baseline upon their removal. The large, vertical current deflections before the initial PKA application are 25-ms I-V pulses. **(B)** Enlargement of the current trace enclosed by the dashed box in A. Single-channel openings are visible  $\sim 10 \text{ s}$  after application of ATP and PKA.